International Journal of Solids and Structures 41 (2004) 2403–2427

INTERNATIONAL JOURNAL OF SOLIDS and STRUCTURES

www.elsevier.com/locate/ijsolstr

Nonlinear vibration and dynamic response of functionally graded plates in thermal environments

Xiao-Lin Huang [a,b], Hui-Shen Shen [a,*]

[a] *School of Civil Engineering and Mechanics, Shanghai Jiao Tong University, 1954 Hua Shan Road, Shanghai 200030, People's Republic of China*

[b] *School of Naval Architecture and Ocean Engineering, Shanghai Jiao Tong University, 1954 Hua Shan Road, Shanghai 200030, People's Republic of China*

Received 11 July 2003; received in revised form 29 October 2003

Abstract

This paper deals with the nonlinear vibration and dynamic response of functionally graded material plates in thermal environments. Heat conduction and temperature-dependent material properties are both taken into account. The temperature field considered is assumed to be a uniform distribution over the plate surface and varied in the thickness direction only. Material properties are assumed to be temperature-dependent, and graded in the thickness direction according to a simple power law distribution in terms of the volume fractions of the constituents. The formulations are based on the higher-order shear deformation plate theory and general von Kármán-type equation, which includes thermal effects. All four edges of the plates are assumed to be simply supported with no in-plane displacements. The equations of motion are solved by an improved perturbation technique to determine nonlinear frequencies and dynamic responses of functionally graded plates. The numerical illustrations concern nonlinear vibration characteristics of functional graded plates with two constituent materials in thermal environments. The results reveal that the temperature field and volume fraction distribution have significant effect on the nonlinear vibration and dynamic response of the functionally graded plate.

Keywords: Functionally graded plate; Nonlinear vibration; Dynamic response; Higher-order shear deformation plate theory; Perturbation technique

1. Introduction

Functionally graded materials (FGMs) have gained considerably attention in engineering community, especially in high temperature applications such as spacecraft and nuclear plants, due to their advantages of being able to withstand severe high temperature gradient while maintain structural integrity. FGMs are microscopically inhomogeneous composites usually made from a mixture of metals and ceramics. By

* Corresponding author.
E-mail address: hsshen@mail.sjtu.edu.cn (H.-S. Shen).

doi:10.1016/j.ijsolstr.2003.11.012

gradually varying the volume fraction of constituent materials, their material properties exhibit a smooth and continuous change from one surface to another, thus eliminating interface problems and mitigating thermal stress concentrations. FGMs were initially designed as thermal barrier materials for aerospace structures and fusion reactors. They are now developed for the general use as structural components in high temperature environments (Liew et al., 2001, 2003).

Since this area is relatively new, published literature on the free and forced vibration of FGM plates is limited and most of them are focused on the cases of the linear problem. Tanigawa et al. (1996) examined transient thermal stress distribution of FGM plates induced by unsteady heat conduction, temperature-dependent material properties were considered. Kim and Noda (2002) discussed transient displacement of FGM plates due to heat flux by a Green's function approach based on the classical laminated plate theory. Cheng and Batra (2000) studied the steady state vibration of a simply supported functionally graded polygonal plate with temperature-independent material properties. Praveen and Reddy (1998) analyzed the nonlinear static and dynamic response of functionally graded ceramic–metal plates in a steady temperature field and subjected to dynamic transverse loads by the finite element method (FEM) based on the first-order shear deformation plate theory (FSDPT). Reddy (2000) developed both theoretical and finite element formulations for thick FGM plates according to the higher-order shear deformation plate theory (HSDPT), and studied the nonlinear dynamic response of FGM plates subjected to suddenly applied uniform pressure. Ng et al. (2000) studied parametric resonance or dynamic stability of simply supported FGM thin plates under harmonic in-plane loading. Yang and Shen (2001) presented the dynamic response of initially stressed FGM thin plates. He et al. (2001) gave the active control of dynamic response of FGM plates bonded with piezoelectric actuators. In their analysis finite element equations based on the classical plate theory were formulated. In the aforementioned studies, however, material properties were considered in a constant temperature environment ($T = 300$ K). Recently, Yang and Shen (2002, 2003) provided vibration characteristic and transient response of shear-deformable functionally graded plates and panels in thermal environments. In their analyses, the material properties were considered to be temperature-dependent and the effect of temperature rise on the dynamic response was reported. In fact, the heat conduction usually occurs (Tanigawa et al., 1996; Liew et al., 2001, 2003; Kim and Noda, 2002), but it is not accounted for in Yang and Shen (2002, 2003). It is because when the material properties are assumed to be functions of temperature and position, and the temperature is also assumed to be a function of position, the problem becomes very difficult.

The present work attempts to solve this problem, that is, to provide analytical solution for nonlinear free and forced vibration of FGM plates in thermal environments. The temperature field is assumed to be constant in the plane and only varies in the thickness direction of the plate. The material properties are assumed to be temperature-dependent, and graded in the thickness direction according to a simple power-law distribution in terms of the volume fractions of the constituents. The formulations, including thermal effects, are based on the higher-order shear deformation plate theory (Reddy, 1984) and general von Kármán-type equations (Shen, 1997, 2002). An improved perturbation technique is employed to determine the nonlinear frequencies and dynamic responses of the FGM plates with two constituent materials. The parametric studies show the effects of volume fraction index and temperature field on natural frequency, nonlinear to linear frequency ratio and dynamic responses of the plate.

2. Theoretical development

Here we consider an FGM plate of length a, width b and thickness h, which is made from a mixture of ceramics and metals. We assume that the composition is varied from the top to the bottom surface, i.e. the top surface ($Z = h/2$) of the plate is ceramic-rich whereas the bottom surface ($Z = -h/2$) is metal-rich. In such a way, the effective material properties P, like Young's modulus E, and thermal expansion coefficient α, can be expressed as

$$P = P_t V_c + P_b V_m \tag{1}$$

in which P_t and P_b denote the temperature-dependent properties of the top and bottom surfaces of the plate, respectively, and may be expressed as a function of temperature (Touloukian, 1967)

$$P = P_0(P_{-1}T^{-1} + 1 + P_1 T + P_2 T^2 + P_3 T^3) \tag{2}$$

where P_0, P_{-1}, P_1, P_2 and P_3 are the coefficients of temperature $T(K)$ and are unique to the constituent materials.

V_c and V_m are the ceramic and metal volume fractions and are related by

$$V_c + V_m = 1 \tag{3}$$

and we assume the volume fraction V_c follows a simple power law as

$$V_c(Z) = \left(\frac{2Z + h}{2h}\right)^N \tag{4}$$

where volume fraction index N dictates the material variation profile through the plate thickness and may be varied to obtain the optimum distribution of component materials.

It is assumed that the effective Young's modulus E and thermal expansion coefficient α are temperature-dependent, whereas the mass density ρ and thermal conductivity κ are independent to the temperature. Poisson's ratio ν depends weakly on temperature change and is assumed to be a constant. From Eqs. (1)–(4), one has

$$E(Z,T) = [E_t(T) - E_b(T)]\left(\frac{2Z + h}{2h}\right)^N + E_b(T) \tag{5a}$$

$$\alpha(Z,T) = [\alpha_t(T) - \alpha_b(T)]\left(\frac{2Z + h}{2h}\right)^N + \alpha_b(T) \tag{5b}$$

$$\rho(Z) = (\rho_t - \rho_b)\left(\frac{2Z + h}{2h}\right)^N + \rho_b \tag{5c}$$

$$\kappa(Z) = (\kappa_t - \kappa_b)\left(\frac{2Z + h}{2h}\right)^N + \kappa_b \tag{5d}$$

We assume that the temperature variation occurs in the thickness direction only and one-dimensional temperature field is assumed to be constant in the XY plane of the plate. In such a case, the temperature distribution along the thickness can be obtained by solving a steady-state heat transfer equation

$$-\frac{d}{dZ}\left[\kappa(Z)\frac{dT}{dZ}\right] = 0 \tag{6}$$

This equation is solved by imposing boundary condition of $T = T_t$ at $Z = h/2$ and $T = T_b$ at $Z = -h/2$. The solution of this equation, by means of polynomial series, is (Javaheri and Eslami, 2002)

$$T(Z) = T_b + (T_t - T_b)\eta(Z) \tag{7}$$

and

$$\eta(Z)=\frac{1}{C}\left[\left(\frac{2Z+h}{2h}\right)-\frac{\kappa_{\mathrm{tb}}}{(N+1)\kappa_{\mathrm{b}}}\left(\frac{2Z+h}{2h}\right)^{N+1}+\frac{\kappa_{\mathrm{tb}}^{2}}{(2N+1)\kappa_{\mathrm{b}}^{2}}\left(\frac{2Z+h}{2h}\right)^{2N+1}-\frac{\kappa_{\mathrm{tb}}^{3}}{(3N+1)\kappa_{\mathrm{b}}^{3}}\left(\frac{2Z+h}{2h}\right)^{3N+1}+\frac{\kappa_{\mathrm{tb}}^{4}}{(4N+1)\kappa_{\mathrm{b}}^{4}}\left(\frac{2Z+h}{2h}\right)^{4N+1}-\frac{\kappa_{\mathrm{tb}}^{5}}{(5N+1)\kappa_{\mathrm{b}}^{5}}\left(\frac{2Z+h}{2h}\right)^{5N+1}\right] \tag{8a}$$

$$C=1-\frac{\kappa_{\mathrm{tb}}}{(N+1)\kappa_{\mathrm{b}}}+\frac{\kappa_{\mathrm{tb}}^{2}}{(2N+1)\kappa_{\mathrm{b}}^{2}}-\frac{\kappa_{\mathrm{tb}}^{3}}{(3N+1)\kappa_{\mathrm{b}}^{3}}+\frac{\kappa_{\mathrm{tb}}^{4}}{(4N+1)\kappa_{\mathrm{b}}^{4}}-\frac{\kappa_{\mathrm{tb}}^{5}}{(5N+1)\kappa_{\mathrm{b}}^{5}} \tag{8b}$$

where $\kappa_{\mathrm{tb}}=\kappa_{\mathrm{t}}-\kappa_{\mathrm{b}}$. In particular, for an isotropic material, Eq. (7) may then be expressed as

$$T(Z)=\frac{T_{\mathrm{t}}+T_{\mathrm{b}}}{2}+\frac{T_{\mathrm{t}}-T_{\mathrm{b}}}{h}Z \tag{9}$$

From Eqs. (5a), (5b) and (7), it can be seen that now E_{t}, E_{b}, α_{t} and α_{b} are all functions of temperature and position.

Suppose the plate is subjected to a transverse dynamic load $q(X,Y,t)$. As usual, the coordinate system has its origin at the corner of the plate on the middle plane. Let $\overline{U}$, $\overline{V}$ and $\overline{W}$ be the plate displacements parallel to a right-hand set of axes (X,Y,Z), where X is longitudinal and Z is perpendicular to the plate. $\overline{\Psi}_x$ and $\overline{\Psi}_y$ are the mid-plane rotations of the normals about the Y- and X-axes, respectively. Reddy (1984) developed a simple higher-order shear deformation plate theory, in which the transverse shear strains are assumed to be parabolically distributed across the plate thickness and which contains the same dependent unknowns ($\overline{U}$, $\overline{V}$, $\overline{W}$, $\overline{\Psi}_x$ and $\overline{\Psi}_y$) as in the first-order shear deformation theory, but no shear correction factors are required. Based on Reddy's higher-order shear deformation plate theory, Shen (1997) derived a set of general von Kármán-type equations which can be expressed in terms of a transverse displacement $\overline{W}$, two rotations $\overline{\Psi}_x$ and $\overline{\Psi}_y$, and stress function $\overline{F}$ defined by $\overline{N}_x=\overline{F}_{,yy}$, $\overline{N}_y=\overline{F}_{,xx}$ and $\overline{N}_{xy}=-\overline{F}_{,xy}$, where a comma denotes partial differentiation with respect to the corresponding coordinates. These general von Kármán-type equations are successfully used in solving many nonlinear problems, e.g. nonlinear bending, post-buckling and nonlinear vibration of shear deformable laminated plates (Shen, 1999, 2000; Huang and Zheng, 2003). Following Shen (1997), we can easily obtain the motion equations of an FGM plate in thermal environments as

$$\widetilde{L}_{11}(\overline{W})-\widetilde{L}_{12}(\overline{\Psi}_x)-\widetilde{L}_{13}(\overline{\Psi}_y)+\widetilde{L}_{14}(\overline{F})-\widetilde{L}_{15}\left(\overline{N}^{\mathrm{T}}\right)-\widetilde{L}_{16}\left(\overline{M}^{\mathrm{T}}\right)=\widetilde{L}(\overline{W},\overline{F})+\widetilde{L}_{17}\left(\ddot{\overline{W}}\right)+I_8\frac{\partial\ddot{\overline{\Psi}}_x}{\partial X}+I_8\frac{\partial\ddot{\overline{\Psi}}_y}{\partial Y}+q \tag{10}$$

$$\widetilde{L}_{21}(\overline{F})+\widetilde{L}_{22}(\overline{\Psi}_x)+\widetilde{L}_{23}(\overline{\Psi}_y)-\widetilde{L}_{24}(\overline{W})-\widetilde{L}_{25}\left(\overline{N}^{\mathrm{T}}\right)=-\frac{1}{2}\widetilde{L}(\overline{W},\overline{W}) \tag{11}$$

$$\widetilde{L}_{31}(\overline{W})+\widetilde{L}_{32}(\overline{\Psi}_x)-\widetilde{L}_{33}(\overline{\Psi}_y)+\widetilde{L}_{34}(\overline{F})-\widetilde{L}_{35}\left(\overline{N}^{\mathrm{T}}\right)-\widetilde{L}_{36}\left(\overline{S}^{\mathrm{T}}\right)=I_9\frac{\partial\ddot{\overline{W}}}{\partial X}+I_{10}\ddot{\overline{\Psi}}_x \tag{12}$$

$$\widetilde{L}_{41}(\overline{W})-\widetilde{L}_{42}(\overline{\Psi}_x)+\widetilde{L}_{43}(\overline{\Psi}_y)+\widetilde{L}_{44}(\overline{F})-\widetilde{L}_{45}\left(\overline{N}^{\mathrm{T}}\right)-\widetilde{L}_{46}\left(\overline{S}^{\mathrm{T}}\right)=I_9\frac{\partial\ddot{\overline{W}}}{\partial Y}+I_{10}\ddot{\overline{\Psi}}_y \tag{13}$$

in which I_j and $\overline{I}_j$ are defined as in Huang and Zheng (2003), and the linear operators $L_{ij}(\ )$ and the nonlinear operator $L(\ )$ are defined as in Shen (2002).

In the above equations, the superposed dots indicate differentiation with respect to time. The forces, moments and higher-order moments caused by temperature rise are defined by

$$\begin{bmatrix} \overline{N}_x^{\mathrm{T}} & \overline{M}_x^{\mathrm{T}} & \overline{P}_x^{\mathrm{T}} \\ \overline{N}_y^{\mathrm{T}} & \overline{M}_y^{\mathrm{T}} & \overline{P}_y^{\mathrm{T}} \\ \overline{N}_{xy}^{\mathrm{T}} & \overline{M}_{xy}^{\mathrm{T}} & \overline{P}_{xy}^{\mathrm{T}} \end{bmatrix} = \int_{-h/2}^{h/2} \begin{bmatrix} A_x \\ A_y \\ A_{xy} \end{bmatrix} \Delta T(Z)(1, Z, Z^3)\, \mathrm{d}Z \tag{14a}$$

$$\begin{bmatrix} \overline{S}_x^{\mathrm{T}} \\ \overline{S}_y^{\mathrm{T}} \\ \overline{S}_{xy}^{\mathrm{T}} \end{bmatrix} = \begin{bmatrix} \overline{M}_x^{\mathrm{T}} \\ \overline{M}_y^{\mathrm{T}} \\ \overline{M}_{xy}^{\mathrm{T}} \end{bmatrix} - \frac{4}{3h^2} \begin{bmatrix} \overline{P}_x^{\mathrm{T}} \\ \overline{P}_y^{\mathrm{T}} \\ \overline{P}_{xy}^{\mathrm{T}} \end{bmatrix} \tag{14b}$$

where $\Delta T(Z) = T(Z) - T_0$ is temperature rise from the reference temperature T_0 at which there are no thermal strains, and

$$\begin{bmatrix} A_x \\ A_y \\ A_{xy} \end{bmatrix} = - \begin{bmatrix} Q_{11} & Q_{12} & Q_{16} \\ Q_{12} & Q_{22} & Q_{26} \\ Q_{16} & Q_{26} & Q_{66} \end{bmatrix} \begin{bmatrix} 1 & 0 \\ 0 & 1 \\ 0 & 0 \end{bmatrix} \begin{bmatrix} \alpha(Z,T) \\ \alpha(Z,T) \end{bmatrix} \tag{15}$$

in which the thermal expansion coefficient α is given in detail in Eq. (5b), and

$$Q_{11} = Q_{22} = \frac{E(Z,T)}{1-v^2}, \quad Q_{12} = \frac{vE(Z,T)}{1-v^2}, \quad Q_{16} = Q_{26} = 0, \quad Q_{44} = Q_{55} = Q_{66} = \frac{E(Z,T)}{2(1+v)} \tag{16}$$

where E is given in detail in Eq. (5a).

It is assumed that all four edges are simply supported with no in-plane displacements. The boundary conditions are

$X = 0, a$:

$$\overline{W} = \overline{\Psi}_y = 0 \tag{17a}$$

$$\overline{U} = 0 \tag{17b}$$

$$\overline{N}_{xy} = 0 \tag{17c}$$

$Y = 0, b$:

$$\overline{W} = \overline{\Psi}_x = 0 \tag{17d}$$

$$\overline{V} = 0 \tag{17e}$$

$$\overline{N}_{xy} = 0 \tag{17f}$$

Note that the stretching–bending coupling gives rise to bending curvatures under the action of in-plane loading, no matter how small these loads may be. In this situation the boundary condition of zero bending moment cannot be incorporated accurately, as reported in Shen (2002). The conditions expressing the immovability conditions (17b) and (17e) are fulfilled on the average sense as (Shen, 2002)

$$\int_0^{\mathrm{b}} \int_0^a \frac{\partial \overline{U}}{\partial X}\, \mathrm{d}X\, \mathrm{d}Y = 0 \tag{18a}$$

$$\int_0^a \int_0^b \frac{\partial \overline{V}}{\partial Y} \, dY \, dX = 0 \tag{18b}$$

In Eq. (18)

$$\frac{\partial \overline{U}}{\partial X} = A_{11}^* \frac{\partial^2 \overline{F}}{\partial Y^2} + A_{12}^* \frac{\partial^2 \overline{F}}{\partial X^2} + \left(B_{11}^* - \frac{4}{3h^2} E_{11}^*\right) \frac{\partial \overline{\Psi}_x}{\partial X} + \left(B_{12}^* - \frac{4}{3h^2} E_{12}^*\right) \frac{\partial \overline{\Psi}_y}{\partial Y} - \frac{4}{3h^2} \left(E_{11}^* \frac{\partial^2 \overline{W}}{\partial X^2} + E_{12}^* \frac{\partial^2 \overline{W}}{\partial Y^2}\right) - \frac{1}{2} \left(\frac{\partial \overline{W}}{\partial X}\right)^2 - \left(A_{11}^* \overline{N}_x^{\mathrm{T}} + A_{12}^* \overline{N}_y^{\mathrm{T}}\right) \tag{19a}$$

$$\frac{\partial \overline{V}}{\partial Y} = A_{22}^* \frac{\partial^2 \overline{F}}{\partial X^2} + A_{12}^* \frac{\partial^2 \overline{F}}{\partial Y^2} + \left(B_{21}^* - \frac{4}{3h^2} E_{21}^*\right) \frac{\partial \overline{\Psi}_x}{\partial X} + \left(B_{22}^* - \frac{4}{3h^2} E_{22}^*\right) \frac{\partial \overline{\Psi}_y}{\partial Y} - \frac{4}{3h^2} \left(E_{21}^* \frac{\partial^2 \overline{W}}{\partial X^2} + E_{22}^* \frac{\partial^2 \overline{W}}{\partial Y^2}\right) - \frac{1}{2} \left(\frac{\partial \overline{W}}{\partial Y}\right)^2 - \left(A_{12}^* \overline{N}_x^{\mathrm{T}} + A_{22}^* \overline{N}_y^{\mathrm{T}}\right) \tag{19b}$$

In Eqs. (19a) and (19b), and what follows, $[A_{ij}^*]$, $[B_{ij}^*]$, $[D_{ij}^*]$, $[E_{ij}^*]$, $[F_{ij}^*]$ and $[H_{ij}^*]$ $(i, j = 1, 2, 6)$ are reduced stiffness matrices, determined through relationships

$$\mathbf{A}^* = \mathbf{A}^{-1}, \quad \mathbf{B}^* = -\mathbf{A}^{-1}\mathbf{B}, \quad \mathbf{D}^* = \mathbf{D} - \mathbf{B}\mathbf{A}^{-1}\mathbf{B}, \quad \mathbf{E}^* = -\mathbf{A}^{-1}\mathbf{E}, \quad \mathbf{F}^* = \mathbf{F} - \mathbf{E}\mathbf{A}^{-1}\mathbf{B}, \quad \mathbf{H}^* = \mathbf{H} - \mathbf{E}\mathbf{A}^{-1}\mathbf{E} \tag{20}$$

where A_{ij}, B_{ij} etc., are the plate stiffnesses, defined in the standard way (Reddy, 1984).

3. Analytical method and asymptotic solutions

Having developed the theory, we will try to solve Eqs. (10)–(13) with boundary condition (17). Before proceeding, it is convenient to first define the following dimensionless quantities for the plate [with γ_{ijk} in Eq. (28) below defined in Shen (2002)].

$$\begin{aligned}
&x = \pi X/a, \quad y = \pi Y/b, \quad z = Z/h, \quad \beta = a/b, \quad W = \overline{W}/[D_{11}^* D_{22}^* A_{11}^* A_{22}^*]^{1/4} \\
&F = \overline{F}/[D_{11}^* D_{22}^*]^{1/2}, \quad (\Psi_x, \Psi_y) = (\overline{\Psi}_x, \overline{\Psi}_y) a/\pi [D_{11}^* D_{22}^* A_{11}^* A_{22}^*]^{1/4}, \quad \gamma_5 = -A_{12}^*/A_{22}^* \\
&\gamma_{14} = [D_{22}^*/D_{11}^*]^{1/2}, \quad \gamma_{24} = [A_{11}^*/A_{22}^*]^{1/2}, \quad (\gamma_{T1}, \gamma_{T2}) = (A_X^{\mathrm{T}}, A_y^{\mathrm{T}}) a^2/\pi^2 [D_{11}^* D_{22}^*]^{1/2} \\
&(\gamma_{T3}, \gamma_{T4}, \gamma_{T6}, \gamma_{T7}) = (D_x^{\mathrm{T}}, D_y^{\mathrm{T}}, F_x^{\mathrm{T}}, F_y^{\mathrm{T}}) a^2/\pi^2 h^2 D_{11}^* \\
&(M_x, M_y, P_x, P_y, M_x^{\mathrm{T}}, M_y^{\mathrm{T}}, P_x^{\mathrm{T}}, P_y^{\mathrm{T}}) \\
&\quad = (\overline{M}_x, \overline{M}_y, 4\overline{P}_x/3h^2, 4\overline{P}_y/3h^2, \overline{M}_x^{\mathrm{T}}, \overline{M}_y^{\mathrm{T}}, 4\overline{P}_x^{\mathrm{T}}/3h^2, 4\overline{P}_y^{\mathrm{T}}/3h^2) a^2/\pi^2 D_{11}^* [D_{11}^* D_{22}^* A_{11}^* A_{22}^*]^{1/4} \\
&\tau = \frac{\pi t}{a}\sqrt{\frac{E_0}{\rho_0}}, \quad \gamma_{170} = -\frac{I_1 E_0 a^2}{\pi^2 \rho_0 D_{11}^*}, \quad \gamma_{171} = \frac{4E_0(I_5 I_1 - I_4 I_2)}{3\rho_0 h^2 I_1 D_{11}^*} \\
&(\gamma_{80}, \gamma_{90}, \gamma_{10}) = (I_8, I_9, I_{10}) \frac{E_0}{\rho_0 D_{11}^*}, \quad \lambda_q = q a^4/\pi^4 D_{11}^* [D_{11}^* D_{22}^* A_{11}^* A_{22}^*]^{1/4}
\end{aligned} \tag{21}$$

in which E_0 and ρ_0 are the reference values of E_b and ρ_b at the room temperature ($T_0 = 300$ K), respectively, and $A_x^{\mathrm{T}}(= A_y^{\mathrm{T}})$, $D_x^{\mathrm{T}}(= D_y^{\mathrm{T}})$, and $F_x^{\mathrm{T}}(= F_y^{\mathrm{T}})$, are defined by

$$\begin{bmatrix} A_x^{\mathrm{T}} & D_x^{\mathrm{T}} & F_x^{\mathrm{T}} \\ A_y^{\mathrm{T}} & D_y^{\mathrm{T}} & F_y^{\mathrm{T}} \end{bmatrix} T_1 = -\int_{-h/2}^{h/2} \begin{bmatrix} A_x \\ A_y \end{bmatrix} \Delta T(Z)(1, Z, Z^3) \, dZ \tag{22}$$

where $T_1 = (T_t + T_b - 2T_0)/2$. We then expand the temperature $T(z)$ in the Taylor series as

$$T(z) = s_0 + s_1 z + s_2 z^2 + s_3 z^3 + s_4 z^4 + s_5 z^5 + \cdots \tag{23}$$

From Eqs. (22) and (23), A_x^{T}, D_x^{T} and F_x^{T} are determined, detail of which can be found in Appendix A. Eqs. (10)–(13) can then be re-written in the following dimensionless form

$$\begin{aligned} &L_{11}(W) - L_{12}(\Psi_x) - L_{13}(\Psi_y) + \gamma_{14}L_{14}(F) - L_{16}(M^{\mathrm{T}}) \\ &\quad = \gamma_{14}\beta^2 L(W,F) + L_{17}(\ddot{W}) + \gamma_{80}\frac{\partial \ddot{\Psi}_x}{\partial x} + \gamma_{80}\beta\frac{\partial \ddot{\Psi}_y}{\partial y} + \lambda_q \end{aligned} \tag{24}$$

$$L_{21}(F) + \gamma_{24}L_{22}(\Psi_x) + \gamma_{24}L_{23}(\Psi_y) - \gamma_{24}L_{24}(W) = -\frac{1}{2}\gamma_{24}\beta^2 L(W,W) \tag{25}$$

$$L_{31}(W) + L_{32}(\Psi_x) - L_{33}(\Psi_y) + \gamma_{14}L_{34}(F) - L_{36}(S^{\mathrm{T}}) = \gamma_{90}\frac{\partial \ddot{W}}{\partial x} + \gamma_{10}\ddot{\Psi}_x \tag{26}$$

$$L_{41}(W) - L_{42}(\Psi_x) + L_{43}(\Psi_y) + \gamma_{14}L_{44}(F) - L_{46}(S^{\mathrm{T}}) = \gamma_{90}\beta\frac{\partial \ddot{W}}{\partial y} + \gamma_{10}\ddot{\Psi}_y \tag{27}$$

where the dimensionless operators $L_{ij}(\ )$ and $L(\ )$ are defined as in Shen (2002).

The boundary conditions of Eq. (17) become

$x = 0$, π:

$$W = \Psi_y = 0 \tag{28a}$$

$$F_{,xy} = 0 \tag{28b}$$

$$\begin{aligned} \int_0^\pi \int_0^\pi \Bigg[&\gamma_{24}^2\beta^2\frac{\partial^2 F}{\partial y^2} - \gamma_5\frac{\partial^2 F}{\partial x^2} + \gamma_{24}\left(\gamma_{511}\frac{\partial \Psi_x}{\partial x} + \gamma_{233}\beta\frac{\partial \Psi_y}{\partial y}\right) - \gamma_{24}\left(\gamma_{611}\frac{\partial^2 W}{\partial x^2} + \gamma_{244}\beta^2\frac{\partial^2 W}{\partial y^2}\right) \\ &- \frac{1}{2}\gamma_{24}\left(\frac{\partial W}{\partial x}\right)^2 + \left(\gamma_{24}^2\gamma_{T1} - \gamma_5\gamma_{T2}\right)T_1 \Bigg] \mathrm{d}x\,\mathrm{d}y = 0 \end{aligned} \tag{28c}$$

$y = 0$, π:

$$W = \Psi_x = 0 \tag{28d}$$

$$F_{,xy} = 0 \tag{28e}$$

$$\begin{aligned} \int_0^\pi \int_0^\pi \Bigg[&\frac{\partial^2 F}{\partial x^2} - \gamma_5\beta^2\frac{\partial^2 F}{\partial y^2} + \gamma_{24}\left(\gamma_{220}\frac{\partial \Psi_x}{\partial x} + \gamma_{522}\beta\frac{\partial \Psi_y}{\partial y}\right) - \gamma_{24}\left(\gamma_{240}\frac{\partial^2 W}{\partial x^2} + \gamma_{622}\beta^2\frac{\partial^2 W}{\partial y^2}\right) \\ &- \frac{1}{2}\gamma_{24}\beta^2\left(\frac{\partial W}{\partial y}\right)^2 + (\gamma_{T2} - \gamma_5\gamma_{T1})T_1 \Bigg] \mathrm{d}y\,\mathrm{d}x = 0 \end{aligned} \tag{28f}$$

We assume that the solutions of Eqs. (24)–(28) can be expressed as

$$\begin{aligned} W(x,y,\tau) &= W^*(x,y) + \widetilde{W}(x,y,\tau) \\ \Psi_x(x,y,\tau) &= \Psi_x^*(x,y) + \widetilde{\Psi}_x(x,y,\tau) \\ \Psi_y(x,y,\tau) &= \Psi_y^*(x,y) + \widetilde{\Psi}_y(x,y,\tau) \\ F(x,y,\tau) &= F^*(x,y) + \widetilde{F}(x,y,\tau) \end{aligned} \tag{29}$$

where $W^*(x,y)$ is an initial deflection due to initial thermal bending moment, and $\widetilde{W}(x,y,\tau)$ is an additional deflection. $\Psi_x^*(x,y)$, $\Psi_y^*(x,y)$ and $F^*(x,y)$ are the mid-plane rotations and stress function corresponding to $W^*(x,y)$. $\widetilde{\Psi}_x(x,y,\tau)$, $\widetilde{\Psi}_y(x,y,\tau)$ and $\widetilde{F}(x,y,\tau)$ are defined analogously to $\Psi_x^*(x,y)$, $\Psi_y^*(x,y)$ and $F^*(x,y)$, but are for $\widetilde{W}(x,y,\tau)$.

Due to the bending-stretching coupling effect in the FGM plate, the thermal pre-load will bring about deflections and bending curvatures which have significant influences on the plate vibration characteristics. To account for this effect, the pre-vibration solutions $W^*(x,y)$, $\Psi_x^*(x,y)$, $\Psi_y^*(x,y)$ and $F^*(x,y)$ are sought at the first step from the following nonlinear equations

$$\begin{aligned} &L_{11}(W^*) - L_{12}(\Psi_x^*) - L_{13}(\Psi_y^*) + \gamma_{14}L_{14}(F^*) - L_{16}(M^{\mathrm{T}}) + \gamma_{14}\beta^2\left(p_x\frac{\partial^2 W^*}{\partial x^2} + p_y\frac{\partial^2 W^*}{\partial y^2}\right) \\ &\quad = \gamma_{14}\beta^2 L(W^*, F^*) \end{aligned} \tag{30}$$

$$L_{21}(F^*) + \gamma_{24}L_{22}(\Psi_x^*) + \gamma_{24}L_{23}(\Psi_y^*) - \gamma_{24}L_{24}(W^*) = -\frac{1}{2}\gamma_{24}\beta^2 L(W^*, W^*) \tag{31}$$

$$L_{31}(W^*) + L_{32}(\Psi_x^*) - L_{33}(\Psi_y^*) + \gamma_{14}L_{34}(F^*) - L_{36}(S^{\mathrm{T}}) = 0 \tag{32}$$

$$L_{41}(W^*) - L_{42}(\Psi_x^*) + L_{43}(\Psi_y^*) + \gamma_{14}L_{44}(F^*) - L_{46}(S^{\mathrm{T}}) = 0 \tag{33}$$

In Eq. (30), p_x and p_y are edge compressive stresses induced by temperature rise with edge restraints. The solutions of Eqs. (30)–(33) can be assumed to be as

$$\begin{aligned} W^*(x,y) &= \sum_{k=1,3,\ldots}\sum_{l=1,3,\ldots} w_{kl}\sin kx \sin ly \\ \Psi_x^*(x,y) &= \sum_{k=1,3,\ldots}\sum_{l=1,3,\ldots} (\psi_x)_{kl}\cos kx \sin ly \\ \Psi_y^*(x,y) &= \sum_{k=1,3,\ldots}\sum_{l=1,3,\ldots} (\psi_y)_{kl}\sin kx \cos ly \\ F^*(x,y) &= -\frac{1}{2}\left(B_{00}^{(0)}y^2 + b_{00}^{(0)}x^2\right) + \sum_{k=1,3,\ldots}\sum_{l=1,3,\ldots} f_{kl}\sin kx \sin ly \end{aligned} \tag{34}$$

We then expand the constant thermal bending moments in the double Fourier sine series as

$$\begin{bmatrix} M_x^{\mathrm{T}} & S_x^{\mathrm{T}} \\ M_y^{\mathrm{T}} & S_y^{\mathrm{T}} \end{bmatrix} = -\begin{bmatrix} M_x^{(0)} & S_x^{(0)} \\ M_y^{(0)} & S_y^{(0)} \end{bmatrix} \sum_{k=1,3,\ldots}\sum_{l=1,3,\ldots} \frac{1}{kl}\sin kx \sin ly \tag{35}$$

Substituting Eqs. (34) and (35) into Eqs. (30)–(33) and applying Galerkin procedure to Eqs. (30) and (31), W_{kl}, $(\psi_x)_{kl}$, $(\psi_y)_{kl}$ and f_{kl} can easily be determined, the detailed expressions are given in Appendix B.

Then an initially stressed FGM plate is under consideration and $\widetilde{W}(x,y,\tau)$, $\widetilde{\Psi}_x(x,y,\tau)$, $\widetilde{\Psi}_y(x,y,\tau)$ and $\widetilde{F}(x,y,\tau)$ satisfy the nonlinear equations

$$L_{11}(\widetilde{W}) - L_{12}(\widetilde{\Psi}_x) - L_{13}(\widetilde{\Psi}_y) + \gamma_{14}L_{14}(\widetilde{F})$$
$$= \gamma_{14}\beta^2 L\left(\widetilde{W} + W^*, \widetilde{F}\right) + L_{17}\left(\ddot{\widetilde{W}}\right) + \gamma_{80}\frac{\partial \ddot{\widetilde{\Psi}}_x}{\partial x} + \gamma_{80}\beta\frac{\partial \ddot{\widetilde{\Psi}}_y}{\partial y} + \lambda_q \tag{36}$$

$$L_{21}(\widetilde{F}) + \gamma_{24}L_{22}(\widetilde{\Psi}_x) + \gamma_{24}L_{23}(\widetilde{\Psi}_y) - \gamma_{24}L_{24}(\widetilde{W}) = -\frac{1}{2}\gamma_{24}\beta^2 L(\widetilde{W} + 2W^*, \widetilde{W}) \tag{37}$$

$$L_{31}(\widetilde{W}) + L_{32}(\widetilde{\Psi}_x) - L_{33}(\widetilde{\Psi}_y) + \gamma_{14}L_{34}(\widetilde{F}) = \gamma_{90}\frac{\partial \ddot{\widetilde{W}}}{\partial x} + \gamma_{10}\ddot{\widetilde{\Psi}}_x \tag{38}$$

$$L_{41}(\widetilde{W}) - L_{42}(\widetilde{\Psi}_x) + L_{43}(\widetilde{\Psi}_y) + \gamma_{14}L_{44}(\widetilde{F}) = \gamma_{90}\beta\frac{\partial \ddot{\widetilde{W}}}{\partial y} + \gamma_{10}\ddot{\widetilde{\Psi}}_y \tag{39}$$

The initial conditions are assumed to be

$$\widetilde{W}|_{\tau=0} = \left.\frac{\partial \widetilde{W}}{\partial \tau}\right|_{\tau=0} = 0 \tag{40a}$$

$$\widetilde{\Psi}_x|_{\tau=0} = \left.\frac{\partial \widetilde{\Psi}_x}{\partial \tau}\right|_{\tau=0} = 0 \tag{40b}$$

$$\widetilde{\Psi}_y|_{\tau=0} = \left.\frac{\partial \widetilde{\Psi}_y}{\partial \tau}\right|_{\tau=0} = 0 \tag{40c}$$

A perturbation technique is now used to solve Eqs. (36)–(39). The essence of this procedure, in the present case, is to assume that

$$\begin{aligned}
\widetilde{W}(x, y, \tilde{\tau}, \varepsilon) &= \sum_{j=1} \varepsilon^j W_j(x, y, \tilde{\tau}) \\
\widetilde{F}(x, y, \tilde{\tau}, \varepsilon) &= \sum_{j=1} \varepsilon^i F_j(x, y, \tilde{\tau}) \\
\widetilde{\Psi}_x(x, y, \tilde{\tau}, \varepsilon) &= \sum_{j=1} \varepsilon^j \Psi_{xj}(x, y, \tilde{\tau}) \\
\widetilde{\Psi}_y(x, y, \tilde{\tau}, \varepsilon) &= \sum_{j=1} \varepsilon^j \Psi_{yj}(x, y, \tilde{\tau}) \\
\lambda_q(x, y, \tilde{\tau}, \varepsilon) &= \sum_{j=1} \varepsilon^j \lambda_j(x, y, \tilde{\tau})
\end{aligned} \tag{41}$$

where ε is a small perturbation parameter. Here we introduce an important parameter $\tilde{\tau} = \varepsilon\tau$, which may be called a slow variable, to improve perturbation procedure for solving nonlinear dynamic problem.

Substituting Eq. (41) into Eqs. (36)–(39), and collecting terms of the same order of ε, a set of perturbation equations is obtained. Applying Galerkin procedure to the second equation of each order, and solving these equations step by step, we obtain asymptotic solutions, up to third-order, as

$$\begin{aligned}
\widetilde{W}(x, y, \tau) = {}& \varepsilon[w_1(\tau) + g_1\ddot{w}_1(\tau)]\sin mx \sin ny + (\varepsilon w_1(\tau))^3[\alpha g_{311}\sin mx \sin ny + g_{331}\sin 3mx \sin ny \\
& + g_{313}\sin mx \sin 3ny] + \mathrm{O}(\varepsilon^4)
\end{aligned} \tag{42}$$

$$\widetilde{\Psi}_x(x,y,\tau) = \varepsilon\Big[g_{11}^{(1,1)}w_1(\tau) + g_2\ddot{w}_1(\tau)\Big]\cos mx\sin ny + g_{12}(\varepsilon w_1(\tau))^2\sin 2mx + (\varepsilon w_1(\tau))^3 \times\Big[\alpha g_{11}^{(1,1)}g_{311}\cos mx\sin ny + g_{11}^{(3,1)}g_{331}\cos 3mx\sin ny + g_{11}^{(1,3)}g_{313}\cos mx\sin 3ny\Big] + \mathrm{O}(\varepsilon^4) \tag{43}$$

$$\widetilde{\Psi}_y(x,y,\tau) = \varepsilon\Big[g_{21}^{(1,1)}w_1(\tau) + g_3\ddot{w}_1(\tau)\Big]\sin mx\cos ny + g_{22}(\varepsilon w_1(\tau))^2\sin 2ny + (\varepsilon w_1(\tau))^3 \times\Big[\alpha g_{21}^{(1,1)}g_{311}\sin mx\cos ny + g_{21}^{(3,1)}g_{331}\sin 3mx\cos ny + g_{21}^{(1,3)}g_{313}\sin mx\cos 3ny\Big] + \mathrm{O}(\varepsilon^4) \tag{44}$$

$$\widetilde{F}(x,y,\tau) = \varepsilon\Big[g_{31}^{(1,1)}w_1(\tau) + g_4\ddot{w}_1(\tau)\Big]\sin mx\sin ny - (\varepsilon w_1(\tau))^2\Big(B_{00}^{(2)}y^2/2 + b_{00}^{(2)}x^2/2 - g_{402}\cos 2ny - g_{420}\cos 2mx\Big) + (\varepsilon w_1(\tau))^3 \times\Big[\alpha g_{31}^{(1,1)}g_{311}\sin mx\sin ny + g_{31}^{(3,1)}g_{331}\sin 3mx\sin ny + g_{31}^{(1,3)}g_{313}\sin mx\sin 3ny\Big] + \mathrm{O}(\varepsilon^4) \tag{45}$$

$$\lambda_q(x,y,\tau) = \varepsilon\Big[g_{41}w_1(\tau) + g_{43}\ddot{w}_1(\tau)\Big]\sin mx\sin ny + (\varepsilon w_1(\tau))^2(g_{441}\cos 2mx + g_{442}\cos 2ny) - \gamma_{14}\beta^2(\varepsilon w_1(\tau))^2\sum_k\sum_l w_{kl}\Big(B_{00}^{(2)}k^2 + b_{00}^{(2)}l^2 - 4k^2n^2g_{402}\cos 2ny - 4l^2m^2g_{420}\cos 2mx\Big) \times\sin kx\sin ly + \bar{\alpha}g_{42}(\varepsilon w_1(\tau))^3\sin mx\sin ny + \mathrm{O}(\varepsilon^4) \tag{46}$$

Note that in Eqs. (42)–(46) $\tilde{\tau}$ is replaced by τ and for the case of free vibration $\alpha = 0$, $\bar{\alpha} = 1$, otherwise $\alpha = 1$, $\bar{\alpha} = 0$. Coefficients $g_{11}^{(i,j)}$, $g_{21}^{(i,j)}$, $g_{31}^{(i,j)}$ $(i,j = 1,3)$ etc. are given in detail in Appendix B.

Multiplying Eq. (46) by $(\sin mx\sin ny)$ and integrating over the plate area, one has

$$g_{43}\frac{\mathrm{d}^2(\varepsilon w_1)}{\mathrm{d}\tau^2} + g_{41}(\varepsilon w_1) + g_{44}(\varepsilon w_1)^2 + \bar{\alpha}g_{42}(\varepsilon w_1)^3 = \bar{\lambda}_q(\tau) \tag{47}$$

in which

$$\bar{\lambda}_q(\tau) = \frac{4}{\pi^2}\int_0^\pi\int_0^\pi \lambda_q(x,y,\tau)\sin mx\sin ny\,\mathrm{d}x\,\mathrm{d}y \tag{48}$$

3.1. Free vibration

When $\bar{\alpha} = 1$, $\lambda_q(\tau) = 0$, Eq. (47) becomes the free vibration equation of the plate. The nonlinear frequency of the plates can be expressed as (Wang, 1992)

$$\omega_{\mathrm{NL}} = \omega_{\mathrm{L}}\left[1 + \frac{9g_{42}g_{41} - 10g_{44}^2}{12g_{41}^2}A^2\right]^{1/2} \tag{49}$$

where $\omega_{\mathrm{L}} = [g_{41}/g_{43}]^{1/2}$ is the dimensionless linear frequency, and $A = \overline{W}_{\max}/h$ is the amplitude to thickness ratio. According to Eq. (21), the corresponding linear frequency can be expressed as $\bar{\omega}_{\mathrm{L}} = \omega_{\mathrm{L}}(\pi/a)(E_0/\rho_0)^{1/2}$, where E_0 and ρ_0 are defined as in Eq. (21).

3.2. Forced vibration

When the forced vibration is under consideration, we take $\bar{\alpha} = 0$. In such a case, Eq. (47) can be re-written as

$$\varepsilon\ddot{w}_1(\tau) + \varepsilon w_1(\tau)\omega_L^2 + \frac{g_{44}}{g_{43}}(\varepsilon w_1(\tau))^2 + O(\varepsilon^4) = \frac{\bar{\lambda}_q(\tau)}{g_{43}} \tag{50}$$

If zero-valued initial conditions prevail, i.e. $w_1(0) = \dot{w}_1(0) = 0$, Eq. (50) may then be solved by using the Runge–Kutta iteration scheme (Pearson, 1986)

$$\begin{aligned}
(\varepsilon w_1)_{i+1} &= (\varepsilon w_1)_i + \Delta\tau(\varepsilon\dot{w}_1)_i + \frac{(\Delta\tau)^2}{6}(L_1 + L_2 + L_3) \\
(\varepsilon\dot{w}_1)_{i+1} &= (\varepsilon\dot{w}_1)_i + \frac{\Delta\tau}{6}(L_1 + 2L_2 + 2L_3 + L_4)
\end{aligned} \tag{51}$$

where $\Delta\tau$ is the time step, and

$$\begin{aligned}
L_1 &= f(\tau_i, (\varepsilon w_1)), \quad L_2 = f\left(\tau_i + \frac{\Delta\tau}{2}, (\varepsilon w_1)_i + \frac{\Delta\tau(\varepsilon\dot{w}_1)_i}{2}\right) \\
L_3 &= f\left(\tau_i + \frac{\Delta\tau}{2}, (\varepsilon w_1)_i + \frac{\Delta\tau(\varepsilon\dot{w}_1)_i}{2} + \frac{(\Delta\tau)^2}{4}L_1\right) \\
L_4 &= f\left(\tau_i + \Delta\tau, (\varepsilon w_1)_i + \Delta\tau(\varepsilon\dot{w}_1)_i + \frac{(\Delta\tau)^2}{2}L_2\right)
\end{aligned} \tag{52}$$

in which

$$f(\tau, x) = -\omega_L^2 x - \frac{g_{44}}{g_{43}}x^2 + \frac{\bar{\lambda}_q(\tau)}{g_{43}} \tag{53}$$

As a result, the solution of Eq. (50) is obtained numerically. Re-substituting it into Eqs. (42)–(46), both displacement and stress function are determined. Next, substituting Eq. (29) into boundary conditions (28), the coefficients $B_{00}^{(0)}$, $b_{00}^{(0)}$, $B_{00}^{(2)}$ and $b_{00}^{(2)}$ are then determined as given in Appendix B.

4. Numerical examples and discussion

Numerical results are presented in this section for FGM plates with two constituent materials. A program was developed for the purpose and many examples have been solved numerically, including the following.

4.1. Comparison studies

To ensure the accuracy and effectiveness of the present method, three test examples were solved for free and forced vibrations of pure isotropic and FGM plates.

Example 1. We first consider the nonlinear free vibration of an isotropic square plate ($a/b = 1.0$, $b/h = 10$ and $\nu = 0.3$) under different thermal loading conditions $\Delta T/T_{cr} = 0$, 0.25, 0.5 and 0.75, where $T_{cr} = 119.783/(\alpha \times 10^4)$ is the critical temperature of the plate (Bhimaraddi and Chandrashekhara, 1993).

The frequency parameter $\Omega = \bar{\omega}_L(a^2/h)[\rho(1-\nu^2)/E]^{1/2}$ and nonlinear to linear frequency ratio ω_{NL}/ω_L are calculated and compared in Table 1 with the results of Bhimaraddi and Chandrashekhara based on the classical plate theory (CPT), first-order shear deformation plate theory (FSDPT) and higher-order shear deformation plate theory (HSDPT).

Example 2. We now consider the free vibration of an FGM square plate made of aluminum oxide and Ti–6Al–4V. The top surface is ceramic-rich, whereas the bottom surface is metal-rich. The material properties, as given in He et al. (2001), are: $E_b = 105.7$ GPa, $\nu_b = 0.2981$, $\rho_b = 4429$ kg/m^3 for Ti–6Al–4V; and $E_t = 320.24$ GPa, $\nu_t = 0.26$, $\rho_t = 3750$ kg/m^3 for aluminum oxide. The FGM plate has $a = b = 0.4$ m and $h = 5$ mm. Table 2 gives the comparison of natural frequency $\bar{\omega}_L$ (Hz) for the two special cases of isotropy, i.e. volume fraction index $N = 0$ and 2000. The FEM results of He et al. (2001) based on the classical plate theory (CPT) and semi-numerical results of Yang and Shen (2002) based on higher-order shear deformation plate theory (HSDPT) are also given for direct comparison.

Table 1
Comparison of natural frequency Ω and nonlinear to linear frequency ratios for an isotropic square plate under different thermal loading conditions ($a/b = 1.0$, $b/h = 10$ and $\nu = 0.3$)

$\Delta T/T_{cr}$	Sources	Ω	$\overline{W}_{max}/h$					
			0.0	0.2	0.4	0.6	0.8	1.0
0.25	HSDPT[a]	4.7624	1.000	1.027	1.105	1.222	1.368	1.535
	FSDPT[a]	4.7232	0.922	1.019	1.097	1.215	1.362	1.529
	CPT[a]	4.9380	1.037	1.063	1.138	1.252	1.395	1.559
	Present	4.7636	1.000	1.027	1.105	1.225	1.374	1.546
0.5	HSDPT	3.8884	1.000	1.041	1.153	1.318	1.517	1.739
	FSDPT	3.8405	0.988	1.029	1.143	1.309	1.509	1.732
	CPT	4.1017	1.055	1.094	1.201	1.360	1.554	1.772
	Present	3.8891	1.000	1.040	1.155	1.323	1.528	1.757
0.75	HSDPT	2.7495	1.000	1.080	1.287	1.569	1.893	2.242
	FSDPT	2.6813	0.975	1.057	1.267	1.553	1.880	2.230
	CPT	3.0437	1.107	1.180	1.372	1.640	1.953	2.293
	Present	2.7492	1.000	1.080	1.291	1.582	1.916	2.275

[a] HSDPT, FSDPT and CPT results all from Bhimaraddi and Chandrashekhara (1993).

Table 2
Comparison of natural frequency $\bar{\omega}_L$ (Hz) for simply supported FGM plates for the two special cases of isotropy

Mode sequence	$N = 0$			$N = 2000$		
	He et al. (2001)	Yang and Shen (2002)	Present	He et al. (2001)	Yang and Shen (2002)	Present
1	144.66	143.96	144.94	268.92	261.46	271.03
2	360.53	360.07	362.04	669.40	653.14	677.04
3	360.53	360.07	362.04	669.40	653.14	677.04
4	569.89	568.88	578.78	1052.49	1044.31	1082.38
5	720.57	718.22	723.06	1338.52	1304.79	1352.24
6	720.57	718.22	723.06	1338.52	1304.79	1352.24
7	919.74	916.40	939.19	1695.23	1694.98	1756.49
8	919.74	916.40	939.19	1695.23	1694.98	1756.49
9	1225.72	1207.09	1226.19	2280.95	2214.34	2294.47
10	1225.72	1207.09	1226.19	2280.95	2214.34	2294.47

Example 3. Finally, the curves of central deflection as functions of time for an FGM square plate subjected to a suddenly applied uniform load with $q_0 = -10^6$ N/m^2 and in thermal environments are plotted and compared in Fig. 1 with the FEM results of Praveen and Reddy (1998) based on first-order shear deformation plate theory (FSDPT). The FGM plate is made of aluminum and alumina. The thickness and side of the square plate are 0.01 and 0.2 m, respectively. The top surface is ceramic-rich, whereas the bottom surface is metal-rich. The temperature is varied only in the thickness direction and determined by the steady-state heat conduction equation with the boundary conditions. A stress free temperature $T_0 = 0$ °C was taken. The material properties adopted are: $E_b = 70$ GPa, $\nu_b = 0.3$, $\rho_b = 2707$ kg/m^3, $\alpha_b = 23.0 \times 10^{-6}$/°C, $\kappa_b = 204$ W/m K for aluminum; and $E_t = 380$ GPa, $\nu_t = 0.3$, $\rho_t = 3800$ kg/m^3, $\alpha_t = 7.4 \times 10^{-6}$/°C, $\kappa_t = 10.4$ W/m K for alumina. In Fig. 1 dimensionless central deflection and time are defined by $W = (\overline{W}E_m h/q_0 a^2)$ and $\tilde{t} = t[E_m/a^2\rho_m]^{1/2}$, respectively.

These three comparisons show that the present results agree well with existing results. Note that in these examples the material properties are assumed to be independent of temperature.

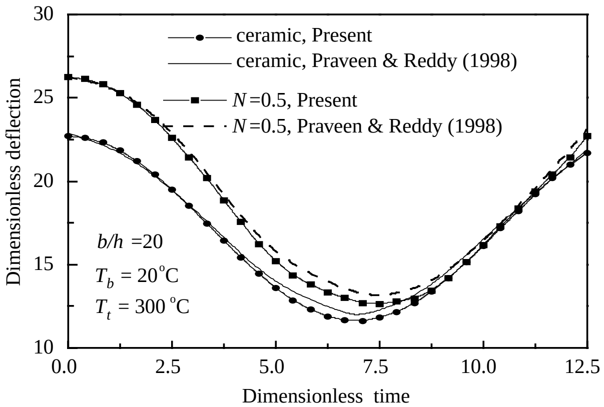

Fig. 1. Comparison of central deflection versus time curves for an FGM square plate subjected to a suddenly applied uniform load and in thermal environments.

Table 3
Temperature-dependent coefficients for ceramic and metals, from Reddy and Chin (1998)

Materials	Proprieties	P_0	P_{-1}	P_1	P_2	P_3	P ($T = 300$ K)
ZrO_2	E (Pa)	244.27e+9	0	−1.371e−3	1.214e−6	−3.681e−10	168.063e+9
	α (1/K)	12.766e−6	0	−1.491e−3	1.006e−5	−6.778e−11	18.591e−6
Ti–6Al–4V	E (Pa)	122.56e+9	0	−4.586e−4	0	0	105.698e+9
	α (1/K)	7.5788e−6	0	6.638e−4	−3.147e−6	0	6.941e−6
Si_3N_4	E (Pa)	348.43e+9	0.0	−3.070e−4	2.160e−7	−8.946e−11	322.2715e+9
	α (1/K)	5.8723e−6	0.0	9.095e−4	0.0	0.0	7.4746e−6
SUS304	E (Pa)	201.04e+9	0.0	3.079e−4	−6.534e−7	0.0	207.7877e+9
	α (1/K)	12.330e−6	0.0	8.086e−4	0.0	0.0	15.321e−6

Table 4
Natural frequency parameter $\Omega = \bar{\omega}_L(a^2/h)[\rho_0(1-\nu^2)/E_0]^{1/2}$ for ZrO_2/Ti–6Al–4V square plates in thermal environments

		Mode				
		(1, 1)	(1, 2)	(2, 2)	(1, 3)	(2, 3)
$T_b = 300$ K	ZrO_2	8.273	19.261	28.962	34.873	43.070
$T_t = 300$ K	0.5	7.139	16.643	25.048	30.174	37.288
	1.0	6.657	15.514	23.345	28.120	34.747
	2.0	6.286	14.625	21.978	26.454	32.659
	Ti–6Al–4V	5.400	12.571	18.903	22.762	28.111
$T_b = 300$ K	ZrO_2	7.868	18.659	28.203	34.015	42.045
$T_t = 400$ K	0.5	6.876	16.264	24.578	29.651	36.664
Temperature-	1.0	6.437	15.202	22.956	27.696	34.236
dependent	2.0	6.101	14.372	21.653	26.113	32.239
	Ti–6Al–4V	5.322	12.455	18.766	22.603	27.921
$T_b = 300$ K	ZrO_2	8.122	19.193	28.986	34.958	43.190
$T_t = 400$ K	0.5	7.154	16.644	25.136	30.136	37.476
Temperature-	1.0	6.592	15.531	23.442	28.273	34.936
independent	2.0	6.238	14.655	22.078	26.605	32.840
	Ti–6Al–4V	5.389	12.620	19.104	22.905	28.261
$T_b = 300$ K	ZrO_2	6.685	16.986	26.073	31.567	39.212
$T_t = 600$ K	0.5	6.123	15.169	23.166	28.041	34.789
Temperature-	1.0	5.819	14.287	21.768	26.342	32.660
dependent	2.0	5.612	13.611	20.652	24.961	30.904
	Ti–6Al–4V	5.118	12.059	18.175	21.898	27.045
$T_b = 300$ K	ZrO_2	7.686	18.749	28.527	34.472	42.713
$T_t = 600$ K	0.5	6.776	16.367	24.859	30.044	37.201
Temperature-	1.0	6.362	15.308	23.216	28.036	34.714
independent	2.0	6.056	14.474	21.896	26.435	32.664
	Ti–6Al–4V	5.284	12.511	18.902	22.784	28.168

4.2. Parametric studies

The close agreements between the present results and those of the referenced solutions as shown in Tables 1 and 2, and Fig. 1 demonstrated the accuracy and effectiveness of the present method. The method was thus deployed to carry out a parametric study to examine the nonlinear vibration and dynamic response of FGM plates in thermal environments. Two sets of material mixture are considered. One is zirconium oxide and titanium alloy, referred to as ZrO_2/Ti–6Al–4V, and the other is silicon nitride and stainless steel, referred to as Si_3N_4/SUS304. The upper surface of these two FGM plates is ceramic-rich and the lower surface is metal-rich. The thickness and side of the square plate are $h = 0.025$ m and $a = 0.2$ m, respectively. The mass density and thermal conductivity are: $\rho = 3000$ kg/m^3, $\kappa = 1.80$ W/m K for ZrO_2; $\rho = 4429$ kg/m^3, $\kappa = 7.82$ W/m K for Ti–6Al–4V; $\rho = 2370$ kg/m^3, $\kappa = 9.19$ W/m K for Si_3N_4; and $\rho = 8166$ kg/m^3, $\kappa = 12.04$ W/m K for SUS304. Young's modulus and thermal expansion coefficient of these materials are assumed to be temperature-dependent and listed in Table 3 (from Reddy and Chin, 1998). Poisson's ratio ν is assumed to be a constant, for ZrO_2/Ti–6Al–4V plate $\nu = 0.3$, and for Si_3N_4/SUS304 one $\nu = 0.28$.

In all examples the deflection mode $(m, n) = (1, 1)$ was used and in Eq. (34) k and l are taken as 1, 3 and 5, and in Eqs. (51) and (52) $\Delta\tau = 2$ μs is taken as the time step for Runge–Kutta iteration method. The temperature field is assumed to vary only in the thickness direction and determined by the steady-state heat

Table 5
Natural frequency parameter $\Omega = \bar{\omega}_L (a^2/h)[\rho_0(1-\nu^2)/E_0]^{1/2}$ for Si_3N_4/SUS304 square plates in thermal environments

		Mode				
		(1, 1)	(1, 2)	(2, 2)	(1, 3)	(2, 3)
$T_b = 300$ K	Si_3N_4	12.495	29.131	43.845	52.822	65.281
$T_t = 300$ K	0.5	8.675	20.262	30.359	36.819	45.546
	1.0	7.555	17.649	26.606	32.081	39.692
	2.0	6.777	15.809	23.806	28.687	35.466
	SUS304	5.405	12.602	18.967	22.850	28.239
$T_b = 300$ K	Si_3N_4	12.397	29.083	43.835	52.822	65.310
$T_t = 400$ K	0.5	8.615	20.215	30.530	36.824	45.575
Temperature-	1.0	7.474	17.607	26.590	32.088	39.721
dependent	2.0	6.693	15.762	23.786	28.686	35.491
	SUS304	5.311	12.539	18.959	22.828	28.246
$T_b = 300$ K	Si_3N_4	12.382	29.243	44.072	53.105	65.559
$T_t = 400$ K	0.5	8.641	20.316	30.682	37.007	45.802
Temperature-	1.0	7.514	17.694	26.717	32.242	39.908
independent	2.0	6.728	15.836	23.893	28.816	35.648
	SUS304	5.335	12.587	19.008	22.908	28.344
$T_b = 300$ K	Si_3N_4	11.984	28.504	43.107	51.998	64.358
$T_t = 600$ K	0.5	8.269	19.783	29.998	36.239	44.901
Temperature-	1.0	7.171	17.213	26.109	31.557	39.114
dependent	2.0	6.398	15.384	23.327	28.185	34.918
	SUS304	4.971	12.089	18.392	22.221	27.557
$T_b = 300$ K	Si_3N_4	12.213	28.976	43.797	52.821	65.365
$T_t = 600$ K	0.5	8.425	20.099	30.458	36.781	45.572
Temperature-	1.0	7.305	17.486	26.506	31.970	39.692
independent	2.0	6.523	15.632	23.685	28.609	35.436
	SUS304	5.104	12.342	18.763	22.658	28.084

Table 6
Effect of volume fraction index N on the nonlinear to linear frequency ratio ω_{NL}/ω_L of FGM square plates in thermal environments ($T_b = 300$ K, $T_t = 400$ K)

	$\overline{W}_{max}/h$					
	0.0	0.2	0.4	0.6	0.8	1.0
ZrO_2/Ti–6Al–4V						
ZrO_2	1.000	1.023	1.087	1.186	1.312	1.461
0.5	1.000	1.023	1.087	1.186	1.312	1.460
1.0	1.000	1.022	1.086	1.183	1.310	1.455
2.0	1.000	1.022	1.084	1.179	1.302	1.444
Ti–6Al–4V	1.000	1.022	1.083	1.177	1.300	1.440
Si_3N_4/SUS304						
Si_3N_4	1.000	1.022	1.084	1.181	1.303	1.446
0.5	1.000	1.022	1.084	1.181	1.302	1.444
1.0	1.000	1.022	1.084	1.180	1.301	1.442
2.0	1.000	1.022	1.082	1.176	1.299	1.440
SUS304	1.000	1.022	1.082	1.172	1.296	1.438

Table 7
Effect of temperature field on the nonlinear to linear frequency ratio ω_{NL}/ω_L of FGM square plates ($N = 2.0$)

	$\overline{W}_{max}/h$					
	0.0	0.2	0.4	0.6	0.8	1.0
ZrO_2/Ti–6Al–4V						
$T_b = 300$ K, $T_t = 300$ K	1.000	1.021	1.082	1.176	1.296	1.436
$T_b = 300$ K, $T_t = 400$ K						
Temperature-dependent	1.000	1.022	1.084	1.179	1.302	1.444
Temperature-independent	1.000	1.022	1.083	1.178	1.300	1.441
$T_b = 300$ K, $T_t = 600$ K						
Temperature-dependent	1.000	1.024	1.091	1.194	1.325	1.477
Temperature-independent	1.000	1.023	1.087	1.183	1.314	1.462
Si_3N_4/SUS304						
$T_b = 300$ K, $T_t = 300$ K	1.000	1.021	1.081	1.174	1.293	1.432
$T_b = 300$ K, $T_t = 400$ K						
Temperature-dependent	1.000	1.022	1.082	1.176	1.299	1.440
Temperature-independent	1.000	1.021	1.082	1.175	1.255	1.437
$T_b = 300$ K, $T_t = 600$ K						
Temperature-dependent	1.000	1.023	1.088	1.188	1.315	1.463
Temperature-independent	1.000	1.023	1.087	1.187	1.313	1.460

conduction equation with the boundary conditions across the plate thickness. Typical results are listed in Tables 4–7 and plotted in Figs. 2–5, for which the dynamic load is assumed to be a suddenly applied uniform load with $q_0 = -50$ MPa.

Tables 4 and 5 show the effect of volume fraction index N on the natural frequency parameter of ZrO_2/Ti–6Al–4V and Si_3N_4/SUS304 plates under three thermal loading conditions: case 1, $T_b = 300$ K, $T_t = 300$ K; case 2, $T_b = 300$ K, $T_t = 400$ K; and case 3, $T_b = 300$ K, $T_t = 600$ K. Temperature-dependent and temperature-independent material properties (values at constant temperature 300 K, as listed in Table 3) are both taken into account. In these two Tables $\Omega = \bar{\omega}_L(a^2/h)[\rho_0(1-\nu^2)/E_0]^{1/2}$, where E_0 and ρ_0 are the reference values of E_b and ρ_b at $T_0 = 300$ K. Then Tables 6 and 7 show, respectively, the effects of volume fraction index N and temperature field on the nonlinear to linear frequency ratios ω_{NL}/ω_L of the same two FGM plates. It can be seen that the natural frequency of the FGM plate decreases with the increase of

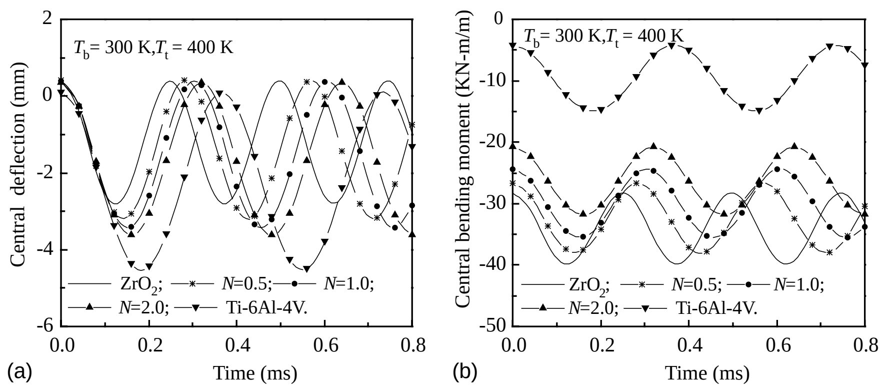

Fig. 2. Effect of volume fraction index N on the dynamic response of ZrO_2/Ti–6Al–4V square plate subjected to a suddenly applied uniform load and in thermal environments. (a) Central deflection versus time, (b) bending moment versus time.

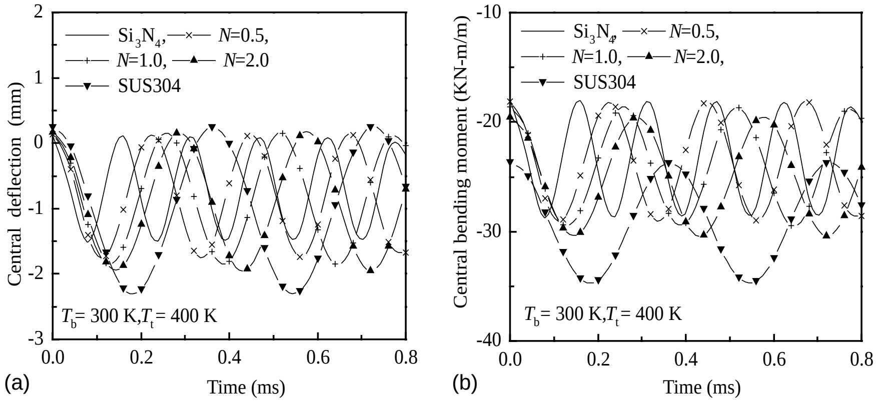

Fig. 3. Effect of volume fraction index N on the dynamic response of Si_3N_4/SUS304 square plate subjected to a suddenly applied uniform load and in thermal environments. (a) Central deflection versus time, (b) bending moment versus time.

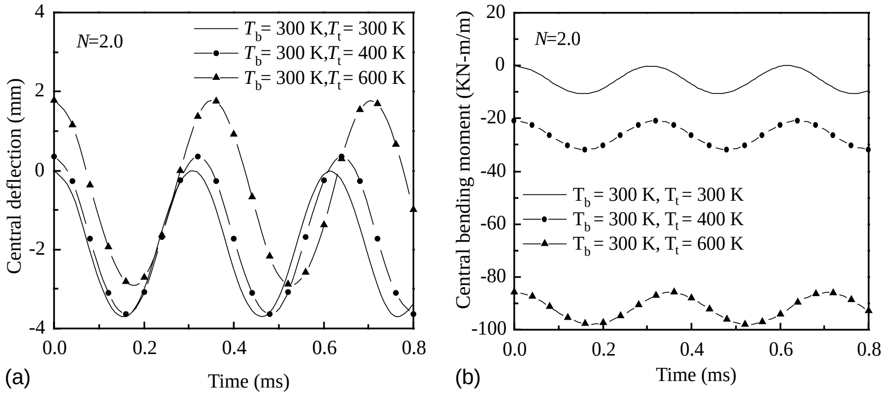

Fig. 4. Effect of temperature field on the dynamic response of ZrO_2/Ti–6Al–4V square plate subjected to a suddenly applied uniform load. (a) Central deflection versus time, (b) bending moment versus time.

volume fraction index N, but it has a small effect on the nonlinear to linear frequency ratios. On the other hand, the temperature rise decreases the natural frequencies but increases the nonlinear to linear frequency ratios. The results show that the FGM plate will have lower natural frequency and slightly higher nonlinear to linear frequency ratios when the temperature-dependent material properties are taken into account.

Figs. 2 and 3 show, respectively, the effect of volume fraction index N on the dynamic response of ZrO_2/Ti–6Al–4V and Si_3N_4/SUS304 plates under thermal environmental condition $T_b = 300$ K and $T_t = 400$ K. It can be seen that the plate deflections are increased by increasing the volume fraction index N. The bending moment is decreased for the ZrO_2/Ti–6Al–4V plate, but it is increased for the Si_3N_4/SUS304 plate when the volume fraction index N is increased.

Figs. 4 and 5 show, respectively, the effect of thermal environmental conditions on the dynamic response of ZrO_2/Ti–6Al–4V and Si_3N_4/SUS304 plates with $N = 2.0$. The results show that both central deflections and bending moments are increased with the increase in temperature. It is also be seen that the greater the temperature rise is, the greater will be the thermally induced initial bending moments.

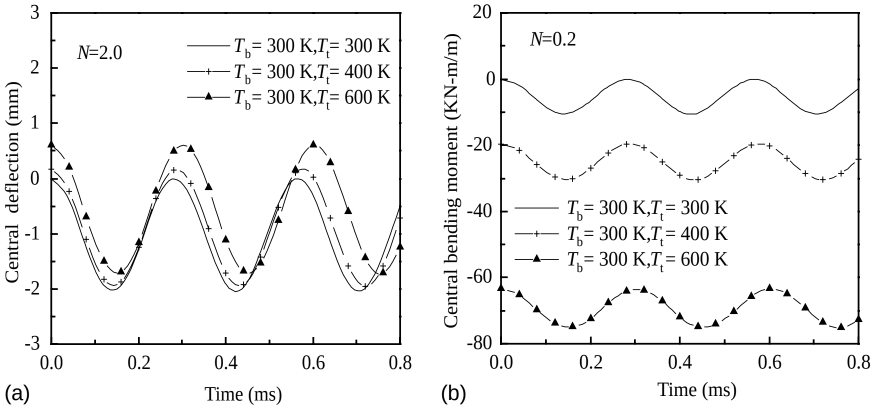

Fig. 5. Effect of temperature field on the dynamic response of Si_3N_4/SUS304 square plate subjected to a suddenly applied uniform load. (a) Central deflection versus time, (b) bending moment versus time.

5. Concluding remarks

The nonlinear vibration and dynamic response for simply supported FGM in thermal environments have been presented. Heat conduction and temperature-dependent material properties are both taken into account. The formulations are based on higher-order shear deformation plate theory and general von Kármán-type equations, and include thermal effects. Analytical solutions have been presented by using an improved perturbation technique. A parametric study for FGM plates with different values of volume fraction index and under different sets of thermal environmental conditions has been carried out. Numerical results show that the natural frequencies are reduced by increasing the volume fraction index N and temperature rise. The results also confirm that the temperature field and the volume fraction distribution have significant effect on the dynamic response of FGM plates.

Acknowledgement

This work is supported in part by the National Natural Science Foundation of China under Grant 50375091. The authors are grateful for this financial support.

Appendix A

In Eq. (23)

$$s_0 = a_0 + 0.5a_1 + (0.5)^{N+1}a_2 + (0.5)^{2N+1}a_3 + (0.5)^{3N+1}a_4 + (0.5)^{4N+1}a_5 + (0.5)^{5N+1}a_6$$

$$s_1 = a_1 + \frac{1}{N+1}(0.5)^{N}a_2 + \frac{1}{2N+1}(0.5)^{2N}a_3 + \frac{1}{3N+1}(0.5)^{3N}a_4 + \frac{1}{4N+1}(0.5)^{4N}a_5 + \frac{1}{5N+1}(0.5)^{5N}a_6$$

$$s_k = \frac{1}{k!}\left[\frac{(N+1-k)!}{(N+1)!}(0.5)^{N-k+1}a_2 + \frac{(2N+1-k)!}{(2N+1)!}(0.5)^{2N-k+1}a_3 + \frac{(3N+1-k)!}{(3N+1)!}(0.5)^{3N-k+1}a_4 \right.$$
$$\left. + \frac{(4N+1-k)!}{(4N+1)!}(0.5)^{4N-k+1}a_5 + \frac{(5N+1-k)!}{(5N+1)!}(0.5)^{5N-k+1}a_6\right] \quad (k = 2\text{–}5) \tag{A.1}$$

and

$$\begin{aligned}
&A_{11}=A_{22}=\frac{1}{1-v^2}\int_{-0.5}^{0.5}E^{(0)}(z)\,\mathrm{d}z,\quad A_{12}=\frac{v}{1-v^2}\int_{-0.5}^{0.5}E^{(0)}(z)\,\mathrm{d}z,\quad A_{16}=A_{26}=0\\
&A_{44}=A_{55}=A_{66}=\frac{1}{2(1+v)}\int_{-0.5}^{0.5}E^{(0)}(z)\,\mathrm{d}z,\quad B_{11}=B_{22}=\frac{1}{1-v^2}\int_{-0.5}^{0.5}E^{(1)}(z)\,\mathrm{d}z\\
&B_{12}=\frac{v}{1-v^2}\int_{-0.5}^{0.5}E^{(1)}(z)\,\mathrm{d}z,\quad B_{16}=B_{26}=0,\quad B_{66}=\frac{1}{2(1+v)}\int_{-0.5}^{0.5}E^{(1)}(z)\,\mathrm{d}z\\
&D_{11}=D_{22}=\frac{1}{1-v^2}\int_{-0.5}^{0.5}E^{(2)}(z)\,\mathrm{d}z,\quad D_{12}=\frac{v}{1-v^2}\int_{-0.5}^{0.5}E^{(2)}(z)\,\mathrm{d}z,\quad D_{16}=D_{26}=0\\
&D_{44}=D_{55}=D_{66}=\frac{1}{2(1+v)}\int_{-0.5}^{0.5}E^{(2)}(z)\,\mathrm{d}z,\quad E_{11}=E_{22}=\frac{1}{1-v^2}\int_{-0.5}^{0.5}E^{(3)}(z)\,\mathrm{d}z\\
&E_{12}=\frac{v}{1-v^2}\int_{-0.5}^{0.5}E^{(3)}(z)\,\mathrm{d}z,\quad E_{16}=E_{26}=0,\quad E_{66}=\frac{1}{2(1+v)}\int_{-0.5}^{0.5}E^{(3)}(z)\,\mathrm{d}z\\
&F_{11}=F_{22}=\frac{1}{1-v^2}\int_{-0.5}^{0.5}E^{(4)}(z)\,\mathrm{d}z,\quad F_{12}=\frac{v}{1-v^2}\int_{-0.5}^{0.5}E^{(4)}(z)\,\mathrm{d}z,\quad F_{16}=F_{26}=0\\
&F_{44}=F_{55}=F_{66}=\frac{1}{2(1+v)}\int_{-0.5}^{0.5}E^{(4)}(z)\,\mathrm{d}z,\quad H_{11}=H_{22}=\frac{1}{1-v^2}\int_{-0.5}^{0.5}E^{(6)}(z)\,\mathrm{d}z\\
&H_{12}=\frac{v}{1-v^2}\int_{-0.5}^{0.5}E^{(6)}(z)\,\mathrm{d}z,\quad H_{16}=H_{26}=0,\quad H_{66}=\frac{1}{2(1+v)}\int_{-0.5}^{0.5}E^{(6)}(z)\,\mathrm{d}z\\
&A_x^{\mathrm{T}}=\frac{2}{(1-v)}\int_{-0.5}^{0.5}f^{(0)}(z)\,\mathrm{d}z,\quad D_x^{\mathrm{T}}=\frac{2}{(1-v)}\int_{-0.5}^{0.5}f^{(1)}(z)\,\mathrm{d}z,\quad F_x^{\mathrm{T}}=\frac{2}{(1-v)}\int_{-0.5}^{0.5}f^{(3)}(z)\,\mathrm{d}z
\end{aligned}\tag{A.2}$$

where

$$\begin{aligned}
&a_0=T_{\mathrm{t}},\quad a_1=\frac{T_{\mathrm{t}}-T_{\mathrm{b}}}{c},\quad a_2=-\frac{T_{\mathrm{t}}-T_{\mathrm{b}}}{c}\cdot\frac{k_{\mathrm{tb}}}{(N+1)k_{\mathrm{b}}},\quad a_3=\frac{T_{\mathrm{t}}-T_{\mathrm{b}}}{c}\cdot\frac{k_{\mathrm{tb}}^2}{(2N+1)k_{\mathrm{b}}^2}\\
&a_4=-\frac{T_{\mathrm{t}}-T_{\mathrm{b}}}{c}\cdot\frac{k_{\mathrm{tb}}^3}{(3N+1)k_{\mathrm{b}}^3},\quad a_5=\frac{T_{\mathrm{t}}-T_{\mathrm{b}}}{c}\cdot\frac{k_{\mathrm{tb}}^4}{(4N+1)k_{\mathrm{b}}^4},\quad a_6=-\frac{T_{\mathrm{t}}-T_{\mathrm{b}}}{c}\cdot\frac{k_{\mathrm{tb}}^5}{(5N+1)k_{\mathrm{b}}^5}\\
&\int_{-0.5}^{0.5}E^{(k)}(z)\,\mathrm{d}z=h^{k+1}\Big\{\frac{e_0}{k+1}[(0.5)^{k+1}-(-0.5)^{k+1}]+\frac{e_1}{k+2}[(0.5)^{k+2}-(-0.5)^{k+2}]\\
&\qquad+\frac{e_2}{k+3}[(0.5)^{k+3}-(-0.5)^{k+3}]+\frac{e_3}{k+4}[(0.5)^{k+4}-(-0.5)^{k+4}]\\
&\qquad+\frac{e_4}{k+5}[(0.5)^{k+5}-(-0.5)^{k+5}]+\frac{e_5}{k+6}[(0.5)^{k+6}-(-0.5)^{k+6}]\Big\}\\
&\int_{-0.5}^{0.5}f^{(k)}(z)\,\mathrm{d}z=h^{k+1}\Big\{\frac{f_0}{k+1}[(0.5)^{k+1}-(-0.5)^{k+1}]+\frac{f_1}{k+2}[(0.5)^{k+2}-(-0.5)^{k+2}]\\
&\qquad+\frac{f_2}{k+3}[(0.5)^{k+3}-(-0.5)^{k+3}]+\frac{f_3}{k+4}[(0.5)^{k+4}-(-0.5)^{k+4}]\\
&\qquad+\frac{f_4}{k+5}[(0.5)^{k+5}-(-0.5)^{k+5}]+\frac{f_5}{k+6}[(0.5)^{k+6}-(-0.5)^{k+6}]\Big\}
\end{aligned}\tag{A.3}$$

in which ($i = 0$–5)

$$e_i = l_i^{(2)} + \sum_{k=0}^{i} l_k^{(1)} d_{(i-k)}, \quad f_i = \sum_{k=0}^{i} u_k a_{i-k}, \quad u_i = \sum_{k=0}^{i} v_k e_{(i-k)} \tag{A.4}$$

and (with $j = 1, 2$)

$$\begin{aligned}
l_0^{(j)} &= g_{-1}^{(j)}/s_0 + g_0^{(j)} + s_0 g_1^{(j)} + s_0^2 g_2^{(j)} + s_0^3 g_3^{(j)} \\
l_1^{(j)} &= c_1 g_{-1}^{(j)} + s_1 g_1^{(j)} + 2 s_0 s_1 g_2^{(j)} + 3 s_0^2 s_1 g_3^{(j)} \\
l_2^{(j)} &= c_2 g_{-1}^{(j)} + s_2 g_1^{(j)} + (s_1^2 + 2 s_0 s_2) g_2^{(j)} + 3(s_0^2 s_2 + s_0 s_1^2) g_3^{(j)} \\
l_3^{(j)} &= c_3 g_{-1}^{(j)} + s_3 g_1^{(j)} + 2(s_0 s_3 + s_1 s_2) g_2^{(j)} + (3 s_0^2 s_3 + 6 s_0 s_1 s_2 + s_1^3) g_3^{(j)} \\
l_4^{(j)} &= s_4 g_1^{(j)} + (s_2^2 + 2 s_0 s_4 + 2 s_1 s_3) g_2^{(j)} + (3 s_0^2 s_4 + 3 s_0 s_2^2 + 6 s_0 s_1 s_3 + 3 s_1^2 s_2) g_3^{(j)} \\
l_5^{(j)} &= s_5 g_1^{(j)} + 2(s_0 s_5 + s_1 s_4 + s_2 s_3) g_2^{(j)} + (3 s_0^2 s_5 + 6 s_0 s_1 s_4 + 6 s_0 s_2 s_3 + 3 s_1 s_2^2 + 3 s_1^3 s_3) g_3^{(j)} \\
c_1 &= -\frac{s_1}{s_0^2}, \quad c_2 = \frac{s_1^2}{s_0^3} - \frac{s_2}{s_0^2}, \quad c_3 = -\frac{s_1^3}{s_0^4} + \frac{2 s_1 s_2}{s_0^3} + \frac{s_3}{s_0^2} \\
d_0 &= (0.5)^N, \quad d_1 = N(0.5)^{N-1}, \quad d_2 = N(N-1)(0.5)^{N-2}/2 \\
d_3 &= N(N-1)(N-2)(0.5)^{N-3}/6, \quad d_4 = N(N-1)(N-2)(N-3)(0.5)^{N-4}/24 \\
d_5 &= N(N-1)(N-2)(N-3)(N-4)(0.5)^{N-5}/120 \\
g_{-1}^{(1)} &= p_0^t p_{-1}^t - p_0^b p_{-1}^b, \quad g_0^{(1)} = p_0^t - p_0^b, \quad g_1^{(1)} = p_0^t p_1^t - p_0^b p_1^b, \quad g_2^{(1)} = p_0^t p_2^t - p_0^b p_2^b \\
g_3^{(1)} &= p_0^t p_3^t - p_0^b p_3^b, \quad g_{-1}^{(2)} = p_0^b p_{-1}^b, \quad g_0^{(2)} = p_0^b, \quad g_1^{(2)} = p_0^b p_1^b, \quad g_2^{(2)} = p_0^b p_2^b, \quad g_3^{(2)} = p_0^b p_3^b
\end{aligned} \tag{A.5}$$

In the above equation p_r^t and p_r^b ($r = -1, 0, 1, 2, 3$) are the coefficients in Eq. (2) for Young's modulus on the top and bottom surfaces. Note that in Eq. (A.4), v_k has the similar form as that of e_i, whereas p_r^t and p_r^b ($r = -1, 0, 1, 2, 3$) are the coefficients in Eq. (2) for thermal expansion coefficient on the top and bottom surfaces.

Appendix B

In Eq. (34)

$$\begin{aligned}
w_{kl} &= \sqrt[3]{-\frac{q_{kl}}{2} + \sqrt{\frac{(q_{kl})^2}{4} + \frac{(p_{kl})^3}{27}}} + \sqrt[3]{-\frac{q_{kl}}{2} - \sqrt{\frac{(q_{kl})^2}{4} + \frac{(p_{kl})^3}{27}}} \\
f_{kl} &= c_{31}^{(k,l)} w_{kl}^2 + c_{32}^{(k,l)} w_{kl} + c_{33}^{(k,l)} \\
(\psi_x)_{kl} &= c_{11}^{(k,l)} w_{kl} + c_{12}^{(k,l)} f_{kl} + c_{13}^{(k,l)}, \quad (\psi_y)_{kl} = c_{21}^{(k,l)} w_{kl} + c_{22}^{(k,l)} f_{kl} + c_{23}^{(k,l)}
\end{aligned} \tag{B.1}$$

where

$$\begin{aligned}
&\left(c_{11}^{(k,l)}, c_{12}^{(k,l)}, c_{13}^{(k,l)}\right) = \frac{1}{b_{32}^{(k,l)}b_{43}^{(k,l)} - b_{42}^{(k,l)}b_{33}^{(k,l)}} \\
&\qquad \times \left(b_{41}^{(k,l)}b_{33}^{(k,l)} - b_{31}^{(k,l)}b_{43}^{(k,l)}, b_{44}^{(k,l)}b_{33}^{(k,l)} - b_{34}^{(k,l)}b_{43}^{(k,l)}, y_3 b_{43}^{(k,l)} - y_4 b_{33}^{(k,l)}\right) \\
&\left(c_{21}^{(k,l)}, c_{22}^{(k,l)}, c_{23}^{(k,l)}\right) = \frac{1}{b_{33}^{(k,l)}b_{42}^{(k,l)} - b_{43}^{(k,l)}b_{32}^{(k,l)}} \\
&\qquad \times \left(b_{41}^{(k,l)}b_{32}^{(k,l)} - b_{31}^{(k,l)}b_{42}^{(k,l)}, b_{44}^{(k,l)}b_{32}^{(k,l)} - b_{34}^{(k,l)}b_{42}^{(k,l)}, y_3 b_{42}^{(k,l)} - y_4 b_{32}^{(k,l)}\right) \\
&\left(c_{31}^{(k,l)}, c_{32}^{(k,l)}, c_{33}^{(k,l)}\right) = -\frac{1}{b_{24}^{(k,l)} + b_{22}^{(k,l)}c_{12}^{(k,l)} + b_{23}^{(k,l)}c_{22}^{(k,l)}} \\
&\qquad \times \left(\frac{16\gamma_{24}kl\beta^2}{3\pi^2}, b_{21}^{(k,l)} + b_{22}^{(k,l)}c_{11}^{(k,l)} + b_{23}^{(k,l)}c_{21}^{(k,l)}, b_{22}^{(k,l)}c_{13}^{(k,l)} + b_{23}^{(k,l)}c_{23}^{(k,l)}\right) \\
&d_1^{(k,l)} = -\left(b_{12}^{(k,l)}c_{12}^{(k,l)}c_{31}^{(k,l)} + b_{13}^{(k,l)}c_{22}^{(k,l)}c_{31}^{(k,l)} + b_{14}^{(k,l)}c_{31}^{(k,l)} - s^{(k,l)}c_{32}^{(k,l)}\right) \Big/ \left(s^{(k,l)}c_{31}^{(k,l)}\right) \\
&d_2^{(k,l)} = \left(b_{11}^{(k,l)} + b_{12}^{(k,l)}c_{11}^{(k,l)} + b_{12}^{(k,l)}c_{12}^{(k,l)}c_{32}^{(k,l)} + b_{13}^{(k,l)}c_{21}^{(k,l)} + b_{13}^{(k,l)}c_{22}^{(k,l)}c_{32}^{(k,l)} + b_{14}^{(k,l)}c_{32}^{(k,l)} - s^{(k,l)}c_{33}^{(k,l)}\right) \Big/ \left(s^{(k,l)}c_{31}^{(k,l)}\right) \\
&d_3^{(k,l)} = \left(b_{12}^{(k,l)}c_{13}^{(k,l)} + b_{13}^{(k,l)}c_{23}^{(k,l)} + b_{14}^{(k,l)}c_{33}^{(k,l)} - y_1\right) \Big/ \left(s^{(k,l)}c_{31}^{(k,l)}\right) \\
&p_{kl} = -d_2^{(k,l)} + \left(d_1^{(k,l)}\right)^2 \Big/ 3, \quad q_{kl} = -d_3^{(k,l)} - \frac{2}{27}\left(d_1^{(k,l)}\right)^2 + \frac{1}{3}d_1^{(k,l)}d_2^{(k,l)} \\
&s^{(k,l)} = \frac{32\gamma_{14}kl\beta^2}{3\pi^2} \\
&b_{11}^{(i,j)} = \gamma_{110}(im)^4 + 2\gamma_{112}(im)^2(jn)^2\beta^2 + \gamma_{114}(jn)^4\beta^4 - \gamma_{14}\beta^2(p_y m^2 + p_x n^2) \\
&b_{12}^{(i,j)} = -[\gamma_{120}(im)^3 + \gamma_{122}im(jn)^2\beta^2] \\
&b_{13}^{(i,j)} = -[\gamma_{131}(im)^2 jn\beta + \gamma_{133}(jn)^3\beta^3] \\
&b_{14}^{(i,j)} = \gamma_{14}[\gamma_{140}(im)^4 + \gamma_{142}(im)^2(jn)^2\beta^2 + \gamma_{144}(jn)^4\beta^4] \\
&b_{21}^{(i,j)} = -\gamma_{24}[\gamma_{240}(im)^4 + \gamma_{242}(im)^2(jn)^2\beta^2 + \gamma_{244}(jn)^4\beta^4] \\
&b_{22}^{(i,j)} = \gamma_{24}[\gamma_{220}(im)^3 + \gamma_{222}(im)(jn)^2\beta^2] \\
&b_{23}^{(i,j)} = \gamma_{24}[\gamma_{231}(im)^2(jn)\beta + \gamma_{233}(jn)^3\beta^3] \\
&b_{24}^{(i,j)} = m^4 + 2\gamma_{212}(im)^2(jn)^2\beta^2 + \gamma_{214}(jn)^4\beta^4 \\
&b_{31}^{(i,j)} = \gamma_{31}(im) - \gamma_{310}(im)^3 - \gamma_{312}(im)(jn)^2\beta^2 \\
&b_{32}^{(i,j)} = \gamma_{31} + r_{320}(im)^2 + \gamma_{322}(jn)^2\beta^2 \\
&b_{33}^{(i,j)} = \gamma_{331}(im)(jn)\beta \\
&b_{34}^{(i,j)} = -\gamma_{24}[\gamma_{220}(im)^3 + \gamma_{222}(im)(jn)^2\beta^2] \\
&b_{41}^{(i,j)} = \gamma_{41}(jn)\beta - \gamma_{411}(im)^2(jn)\beta - \gamma_{413}(jn)^3\beta^3 \\
&b_{42}^{(i,j)} = \gamma_{331}(im)(jn)\beta \\
&b_{43}^{(i,j)} = \gamma_{41} + r_{430}(im)^2 + \gamma_{432}(jn)^2\beta^2 \\
&b_{44}^{(i,j)} = -\gamma_{14}[\gamma_{231}(im)^2(jn)\beta + \gamma_{233}(jn)^3\beta^3] \\
&y_1^{(k,l)} = M_x^{(0)}k/l + \beta^2 M_y^{(0)}l/k, \quad y_3^{(k,l)} = -S_x^{(0)}/l, \quad y_4^{(k,l)} = \beta S_y^{(0)}/k
\end{aligned} \tag{B.2}$$

In Eqs. (35)

$$\begin{bmatrix} M_x^{(0)} & S_x^{(0)} \\ M_y^{(0)} & S_y^{(0)} \end{bmatrix} = \frac{16hT_1}{\pi^2[D_{11}^* D_{22}^* A_{11}^* A_{22}^*]^{1/4}} \begin{bmatrix} \gamma_{T3} & \gamma_{T3} - \gamma_{T6} \\ \gamma_{T4} & \gamma_{T4} - \gamma_{T7} \end{bmatrix} \tag{B.3}$$

In Eqs. (42)–(46) (with $i, j = 1, 3$)

$$\begin{aligned} B_{00}^{(0)} = & -\frac{1}{(\gamma_5^2 - \gamma_{24}^2)\beta^2} \Bigg\{ [(\gamma_{24}^2 \gamma_{T1} - \gamma_5 \gamma_{T2}) + \gamma_5(\gamma_{T2} - \gamma_5 \gamma_{T1})] T_1 \\ & - \frac{4}{\pi^2} \sum_{k=1,3,\dots} \sum_{l=1,3,\dots} \frac{1}{kl} \left[(\gamma_5^2 - \gamma_{24}^2) n^2 \beta^2 f_{kl} - \gamma_{24}(\gamma_{511} + \gamma_5 \gamma_{220}) m \psi_{kl} \right. \\ & \left. - \gamma_{24}(\gamma_{233} + \gamma_5 \gamma_{522}) n \beta \psi_{kl} + \gamma_{24}(\gamma_{611} m^2 + \gamma_{244} n^2 \beta^2) w_{kl} + \gamma_5 \gamma_{24}(\gamma_{240} m^2 + \gamma_{622} n^2 \beta^2) w_{kl} \right] \Bigg\} \end{aligned}$$

$$\begin{aligned} b_{00}^{(0)} = & -\frac{1}{(\gamma_5^2 - \gamma_{24}^2)} \Bigg\{ [\gamma_5(\gamma_{24}^2 \gamma_{T1} - \gamma_5 \gamma_{T2}) + \gamma_{24}^2(\gamma_{T2} - \gamma_5 \gamma_{T1})] T_1 \\ & - \frac{4}{\pi^2} \sum_{k=1,3,\dots} \sum_{l=1,3,\dots} \frac{1}{kl} \left[(\gamma_5^2 - \gamma_{24}^2) m^2 f_{kl} - \gamma_{24}(\gamma_5 \gamma_{511} + \gamma_{24}^2 \gamma_{220}) m \psi_{kl} \right. \\ & \left. - \gamma_{24}(\gamma_5 \gamma_{233} + \gamma_{24}^2 \gamma_{522}) n \beta \psi_{kl} + \gamma_5 \gamma_{24}(\gamma_{611} m^2 + \gamma_{244} n^2 \beta^2) w_{kl} + \gamma_{24}^3(\gamma_{240} m^2 + \gamma_{622} n^2 \beta^2) w_{kl} \right] \Bigg\} \end{aligned}$$

$$g_{11}^{(i,j)} = \frac{k_{23}^{(i,j)} k_{31}^{(i,j)} - k_{33}^{(i,j)} k_{21}^{(i,j)}}{k_{22}^{(i,j)} k_{33}^{(i,j)} - k_{32}^{(i,j)} k_{23}^{(i,j)}}, \quad g_{21}^{(i,j)} = \frac{k_{22}^{(i,j)} k_{31}^{(i,j)} - k_{32}^{(i,j)} k_{21}^{(i,j)}}{k_{23}^{(i,j)} k_{32}^{(i,j)} - k_{33}^{(i,j)} k_{22}^{(i,j)}}$$

$$g_{31}^{(i,j)} = a_1^{(i,j)} + b_1^{(i,j)} g_{11}^{(i,j)} + c_1^{(i,j)} g_{21}^{(i,j)}$$

$$g_{402} = \frac{\gamma_{24} m^2 n^2 \beta^2}{2\left(16\gamma_{214} n^4 \beta^4 + \frac{64\gamma_{14}\gamma_{24}\gamma_{223}^2 n^6 \beta^6}{\gamma_{41} + 4\gamma_{432} n^2 \beta^2}\right)}, \quad g_{420} = \frac{\gamma_{24} m^2 n^2 \beta^2}{2\left(16 m^4 + \frac{64\gamma_{14}\gamma_{24}\gamma_{220}^2 m^6}{\gamma_{31} + 4\gamma_{320} m^2}\right)}$$

$$g_{12} = -\frac{8\gamma_{220}\gamma_{14} m^3}{\gamma_{31} + 4\gamma_{320} m^2} . g_{420}, \quad g_{22} = -\frac{8\gamma_{233}\gamma_{14} n^3 \beta^3}{\gamma_{41} + 4\gamma_{432} n^2 \beta^2} \cdot g_{402}$$

$$g_{441} = 8 g_{12} \gamma_{120} m^3 + 16 g_{420} \gamma_{14} \gamma_{140} m^4 + g_{31}^{(1,1)} \gamma_{14} \beta^2 m^2 n^2$$

$$g_{442} = 8 g_{22} \gamma_{133} n^3 \beta^3 + 16 g_{420} \gamma_{14} \gamma_{144} n^4 \beta^4 + g_{31}^{(1,1)} \gamma_{14} \beta^2 m^2 n^2$$

$$B_{00}^{(2)} = \frac{\gamma_{24}(m^2 + \gamma_5 n^2 \beta^2)}{8(\gamma_5^2 - \gamma_{24}^2)\beta^2}, \quad b_{00}^{(2)} = \frac{\gamma_{24}(\gamma_5 m^2 + \gamma_{24}^2 n^2 \beta^2)}{8(\gamma_5^2 - \gamma_{24}^2)}$$

$$g_{311} = \frac{\gamma_{14}\beta^2(m^2 B_{00}^{(2)} + n^2 b_{00}^{(2)}) - 2m^2 n^2 \gamma_{14} \beta^2 (g_{402} + g_{420})}{k_{11}^{(1,1)} + k_{12}^{(1,1)} g_{11}^{(1,1)} + k_{13}^{(1,1)} g_{21}^{(1,1)} - \gamma_{14}\beta^2 \left(m^2 B_{00}^{(0)} + n^2 b_{00}^{(0)} + s^{(1,1)}\right)}$$

$$g_{331} = \frac{2\gamma_{14} m^2 n^2 \beta^2}{k_{11}^{(3,1)} + k_{12}^{(3,1)} g_{11}^{(3,1)} + k_{13}^{(3,1)} g_{21}^{(3,1)} - \gamma_{14}\beta^2 \left(9m^2 B_{00}^{(0)} + n^2 b_{00}^{(0)} + s^{(3,1)}\right)} g_{420}$$

$$g_{313} = \frac{2\gamma_{14} m^2 n^2 \beta^2}{k_{11}^{(1,3)} + k_{12}^{(1,3)} g_{11}^{(1,3)} + k_{13}^{(1,3)} g_{21}^{(1,3)} - \gamma_{14}\beta^2 \left(m^2 B_{00}^{(0)} + 9n^2 b_{00}^{(0)} + s^{(1,3)}\right)} g_{402}$$

$$g_1 = \frac{-b_2 k_{13}^{(1,1)} \left(k_{12}^{(1,1)} k_{33}^{(1,1)} - k_{32}^{(1,1)} k_{13}^{(1,1)}\right) + b_3 k_{13}^{(1,1)} \left(k_{12}^{(1,1)} k_{23}^{(1,1)} - k_{22}^{(1,1)} k_{13}^{(1,1)}\right)}{\left(k_{11}^{(1,1)} k_{23}^{(1,1)} - k_{21}^{(1,1)} k_{13}^{(1,1)}\right)\left(k_{12}^{(1,1)} k_{33}^{(1,1)} - k_{32}^{(1,1)} k_{13}^{(1,1)}\right) - \left(k_{11}^{(1,1)} k_{33}^{(1,1)} - k_{31}^{(1,1)} k_{13}^{(1,1)}\right)\left(k_{12}^{(1,1)} k_{23}^{(1,1)} - k_{22}^{(1,1)} k_{13}^{(1,1)}\right)}$$

$$g_2 = \frac{-b_2 k_{13}^{(1,1)}\left(k_{11}^{(1,1)}k_{33}^{(1,1)} - k_{31}^{(1,1)}k_{13}^{(1,1)}\right) + b_3 k_{13}^{(1,1)}\left(k_{11}^{(1,1)}k_{23}^{(1,1)} - k_{21}^{(1,1)}k_{13}^{(1,1)}\right)}{\left(k_{12}^{(1,1)}k_{23}^{(1,1)} - k_{22}^{(1,1)}k_{13}^{(1,1)}\right)\left(k_{11}^{(1,1)}k_{33}^{(1,1)} - k_{31}^{(1,1)}k_{13}^{(1,1)}\right) - \left(k_{12}^{(1,1)}k_{33}^{(1,1)} - k_{32}^{(1,1)}k_{13}^{(1,1)}\right)\left(k_{11}^{(1,1)}k_{23}^{(1,1)} - k_{21}^{(1,1)}k_{13}^{(1,1)}\right)}$$

$$g_3 = -\frac{k_{11}^{(1,1)}g_1 + k_{12}^{(1,1)}g_2}{k_{13}^{(1,1)}}, \quad g_4 = a_1^{(1,1)}g_1 + b_1^{(1,1)}g_2 + c_1^{(1,1)}g_3$$

$$g_{41} = k_{11}^{(1,1)} + k_{12}^{(1,1)}g_{11}^{(1,1)} + k_{13}^{(1,1)}g_{21}^{(1,1)} - \gamma_{14}\beta^2\left(m^2 B_{00}^{(0)} + n^2 b_{00}^{(0)} + s^{(1,1)}\right)$$

$$g_{42} = -\gamma_{14}\beta^2\left[m^2 B_{00}^{(2)} + n^2 b_{00}^{(2)} - 2m^2n^2(g_{402} + g_{420})\right]$$

$$g_{43} = -\left(\gamma_{170} - \gamma_{171}m^2 - \gamma_{171}n^2\beta^2 - \gamma_{80}mg_{11}^{(1,1)} - \gamma_{80}n\beta g_{21}^{(1,1)}\right)$$

$$g_{44} = -\frac{2}{\pi^2 mn}\left[g_{441}(1-\cos m\pi)\left(\frac{2}{3}+\frac{1}{3}\cos 3m\pi - \cos m\pi\right) + g_{442}(1-\cos n\pi)\left(\frac{2}{3}+\frac{1}{3}\cos 3n\pi - \cos n\pi\right)\right]$$
$$- \gamma_{14}\beta^2\left(B_{00}^{(2)}m^2 + b_{00}^{(2)}n^2\right)w_{mn}$$

$$B_{00}^{(2)} = \frac{\gamma_{24}\left(m^2 + \gamma_5 n^2\beta^2\right)}{8(\gamma_5^2 - \gamma_{24}^2)\beta^2}, \quad b_{00}^{(2)} = \frac{\gamma_{24}\left(\gamma_5 m^2 + \gamma_{24}^2 n^2\beta^2\right)}{8(\gamma_5^2 - \gamma_{24}^2)} \tag{B.4}$$

where

$$s^{(m,n)} = \frac{2}{\pi^2}\sum_{k=1,3,\ldots}\sum_{l=1,3,\ldots}\left[2(k^2n^2 + l^2m^2)\left(\frac{1}{k} - \frac{1}{2k+4m} - \frac{1}{2k-4im}\right)\left(\frac{1}{l} - \frac{1}{2l+4n} - \frac{1}{2l-4n}\right)\right.$$
$$\left. - klmn\left(\frac{1}{2m+k} + \frac{1}{2m-k}\right)\left(\frac{1}{2n+l} + \frac{1}{2n-l}\right)\left(g_{13}^{(k,l)}w_{kl} + f_{kl}\right)\right] \tag{B.5}$$

$$b_2 = \gamma_{90}m + \gamma_{10}g_{11}^{(1,1)}, \quad b_3 = \gamma_{90}n\beta + \gamma_{10}g_{21}^{(1,1)}$$

In the above equations

$$k_{11}^{(i,j)} = \gamma_{110}(im)^4 + 2\gamma_{112}(im)^2(jn)^2\beta^2 + \gamma_{114}(jn)^4\beta^4$$
$$+ \gamma_{14}\left[\gamma_{140}(im)^4 + \gamma_{142}(im)^2(jn)^2\beta^2 + \gamma_{144}(jn)^4\beta^4\right]a_1^{(i,j)} - \alpha_1\gamma_{14}\beta^2\left(B_{00}^{(0)}m^2 + b_{00}^{(0)}n^2\right)$$
$$k_{12}^{(i,j)} = -\left[\gamma_{120}(im)^3 + \gamma_{122}im(jn)^2\beta^2\right] + \gamma_{14}\left[\gamma_{140}(im)^4 + \gamma_{142}(im)^2(jn)^2\beta^2 + \gamma_{144}(jn)^4\beta^4\right]b_1^{(i,j)}$$
$$k_{13}^{(i,j)} = -\left[\gamma_{131}(im)^2jn\beta + \gamma_{133}(jn)^3\beta^3\right] + \gamma_{14}\left[\gamma_{140}(im)^4 + \gamma_{142}(im)^2(jn)^2\beta^2 + \gamma_{144}(jn)^4\beta^4\right]c_1^{(i,j)}$$
$$k_{21}^{(i,j)} = \gamma_{31}im - \gamma_{310}(im)^3 - \gamma_{312}im(jn)^2\beta^2 - \gamma_{14}\left[\gamma_{220}(im)^3 + \gamma_{222}(im)(jn)^2\beta^2\right]a_1^{(i,j)}$$
$$k_{22}^{(i,j)} = \gamma_{31} + r_{320}(im)^2 + \gamma_{322}(jn)^2\beta^2 - \gamma_{14}\left[\gamma_{220}(im)^3 + \gamma_{222}(im)(jn)^2\beta^2\right]b_1^{(i,j)} \tag{B.6}$$
$$k_{23}^{(i,j)} = \gamma_{331}(im)(jn)\beta - \gamma_{14}\left[\gamma_{220}(im)^3 + \gamma_{222}(im)(jn)^2\beta^2\right]c_1^{(i,j)}$$
$$k_{31}^{(i,j)} = \gamma_{41}jn\beta - \gamma_{411}(im)^2jn\beta - \gamma_{413}(jn)^3\beta^3 - \gamma_{14}\left[\gamma_{231}(im)^2(jn)\beta + \gamma_{233}(jn)^3\beta^3\right]a_1^{(i,j)}$$
$$k_{32}^{(i,j)} = \gamma_{331}(im)(jn)\beta - \gamma_{14}\left[\gamma_{231}(im)^2(jn)\beta + \gamma_{233}(jn)^3\beta^3\right]b_1^{(i,j)}$$
$$k_{33}^{(i,j)} = \gamma_{41} + r_{430}(im)^2 + \gamma_{432}(jn)^2\beta^2 - \gamma_{14}\left[\gamma_{231}(im)^2(jn)\beta + \gamma_{233}(jn)^3\beta^3\right]c_1^{(i,j)}$$

in which, when w_{kl}, ψ_{xkl}, ψ_{ykl} and f_{kl} are considered, $\alpha_1 = 1$, otherwise $\alpha_1 = 0$, and

$$\begin{aligned}
a_1^{(i,j)} &= -\frac{\gamma_{24}}{m^4 + 2\gamma_{212}(im)^2(jn)^2\beta^2 + \gamma_{214}(jn)^4\beta^4}\left\{\gamma_{240}(im)^4. + \gamma_{242}(im)^2(jn)^2\beta^2 + \gamma_{244}(jn)^4\beta^4\right.\\
&\quad + \frac{2\beta^2}{\pi^2}\sum_{k=1,3\ldots}\sum_{l=1,3,\ldots}\left[2(k^2n^2 + l^2m^2)\left(\frac{1}{k} - \frac{1}{2k+4m} - \frac{1}{2k-4m}\right)\left(\frac{1}{l} - \frac{1}{2l+4n} - \frac{1}{2l-4n}\right)\right.\\
&\quad \left.\left. - mnkl\left(\frac{1}{2m+k} + \frac{1}{2m-k}\right)\left(\frac{1}{2n+l} - \frac{1}{2n-l}\right)\right]w_{kl}\right\}\\
b_1^{(i,j)} &= -\frac{\gamma_{24}[\gamma_{220}(im)^3 + \gamma_{222}(im)(jn)^2\beta^2]}{m^4 + 2\gamma_{212}(im)^2(jn)^2\beta^2 + \gamma_{214}(jn)^4\beta^4}\\
c_1^{(i,j)} &= -\frac{\gamma_{24}[\gamma_{231}(im)^2(jn)\beta + \gamma_{233}(jn)^3\beta^3]}{m^4 + 2\gamma_{212}(im)^2(jn)^2\beta^2 + \gamma_{214}(jn)^4\beta^4}
\end{aligned} \tag{B.7}$$

References

Bhimaraddi, A., Chandrashekhara, K., 1993. Nonlinear vibrations of heated antisymmetric angle-ply laminated plates. International Journal of Solids and Structures 30, 1255–1268.

Cheng, Z.-Q., Batra, R.C., 2000. Exact correspondence between eigenvalues of membranes and functionally graded simply supported polygonal plates. Journal of Sound and Vibration 229, 879–895.

He, X.Q., Ng, T.Y., Sivashanker, S., Liew, K.M., 2001. Active control of FGM plates with integrated piezoelectric sensors and actuators. International Journal of Solids and Structures 38, 1641–1655.

Huang, X.-L., Zheng, J.-J., 2003. Nonlinear vibration and dynamic response of simply supported shear deformable laminated plates on elastic foundations. Engineering Structures 25, 1107–1119.

Javaheri, R., Eslami, M.R., 2002. Thermal buckling of functionally graded plates. AIAA Journal 40, 162–169.

Kim, K.-S., Noda, N., 2002. A Green's function approach to the deflection of a FGM plate under transient thermal loading. Archive of Applied Mechanics 72, 127–137.

Liew, K.M., He, X.Q., Ng, T.Y., Sivashanker, S., 2001. Active control of FGM plates subjected to a temperature gradient: modelling via finite element method based on FSDT. International Journal for Numerical Methods in Engineering 52, 1253–1271.

Liew, K.M., He, X.Q., Ng, T.Y., Kitipornchai, S., 2003. Finite element piezothermoelasticity analysis and the active control of FGM plates with integrated piezoelectric sensors and actuators. Computational Mechanics 31, 350–358.

Ng, T.Y., Lam, K.Y., Liew, K.M., 2000. Effects of FGM materials on the parametric resonance of plate structures. Computer Methods in Applied Mechanics and Engineering 190, 953–962.

Pearson, C.E., 1986. Numerical Methods in Engineering and Science. Van Nostrand Reinhold Company Inc.

Praveen, G.N., Reddy, J.N., 1998. Nonlinear transient thermoelastic analysis of functionally graded ceramic–metal plates. International Journal of Solids and Structures 35, 4457–4476.

Reddy, J.N., 1984. A refined nonlinear theory of plates with transverse shear deformation. International Journal of Solids and Structures 20, 881–896.

Reddy, J.N., 2000. Analysis of functionally graded plates. International Journal for Numerical Methods in Engineering 47, 663–684.

Reddy, J.N., Chin, C.D., 1998. Thermomechanical analysis of functionally graded cylinders and plates. Journal of Thermal Stresses 21, 593–629.

Shen, H.-S., 1997. Kármán-type equations for a higher-order shear deformation plate theory and its use in the thermal postbuckling analysis. Applied Mathematics and Mechanics 18, 1137–1152.

Shen, H.-S., 1999. Thermal postbuckling of imperfect shear deformable laminated plates on two-parameter elastic foundations. Mechanics of Composite Materials and Structures 6, 207–228.

Shen, H.-S., 2000. Non-linear bending of shear deformable laminated plates under lateral pressure and thermal loading and resting on elastic foundations. Journal of Strain Analysis for Engineering Design 35, 93–108.

Shen, H.-S., 2002. Nonlinear bending response of functionally graded plates subjected to transverse loads and in thermal environments. International Journal of Mechanical Sciences 44, 561–584.

Tanigawa, Y., Akai, T., Kawamura, R., Oka, N., 1996. Transient heat conduction and thermal stress problems of a nonhomogeneous plate with temperature-dependent material properties. Journal of Thermal Stresses 19, 77–102.

Touloukian, Y.S., 1967. Thermophysical Properties of High Temperature Solid Materials. MacMillan, New York.

Wang, H.-Q., 1992. Nonlinear Vibration (in Chinese) Higher Education Press.

Yang, J., Shen, H.-S., 2001. Dynamic response of initially stressed functionally graded rectangular thin plates. Composite Structures 54, 497–508.

Yang, J., Shen, H.-S., 2002. Vibration characteristic and transient response of shear-deformable functionally graded plates in thermal environments. Journal of Sound and Vibration 255, 579–602.

Yang, J., Shen, H.-S., 2003. Free vibration and parametric resonance of shear deformable functionally graded cylindrical panels. Journal of Sound and Vibration 261, 871–893.